RadioGraphics

From the Archives of the AFIP

Central Nervous System Infections Associated with Human Immunodeficiency Virus Infection: Radiologic-Pathologic Correlation[1]

Alice B. Smith, Lt Col, USAF, MC • James G. Smirniotopoulos, MD
Elisabeth J. Rushing, COL, MC, USA

CME FEATURE

See accompanying test at http://www.rsna.org/education/rg_cme.html

LEARNING OBJECTIVES FOR TEST 6

After reading this article and taking the test, the reader will be able to:

- Describe the clinical and pathologic features of CNS infections in patients with HIV infection.
- Identify the imaging patterns of CNS infections in patients with HIV infection.
- Discuss the differential diagnosis of CNS infections in patients with HIV infection.

TEACHING POINTS

See last page

Diseases of the central nervous system (CNS) in patients infected with the human immunodeficiency virus (HIV) result directly from HIV itself or from a variety of opportunistic agents. These infections include progressive multifocal leukoencephalopathy, toxoplasmosis, and cryptococcosis. A resurgence of tuberculosis and neurosyphilis has also been documented. Mass lesions, meningoencephalitis, demyelination, atrophy, and vascular lesions are the commonly encountered imaging findings. The introduction of highly active antiretroviral therapy (HAART) has improved both the clinical and radiologic findings in HIV-infected patients and reduced the number of opportunistic infections. In countries that use HAART, AIDS (acquired immunodeficiency syndrome) dementia complex is becoming the most common neurologic complication of HIV infection, whereas opportunistic infections are still the major cause of neurologic complications in patients from countries that do not commonly use HAART. Immune reconstitution inflammatory syndrome, which occurs in some patients in the weeks to months after the institution of HAART, may alter the typical imaging appearance of infectious diseases involving the CNS. Knowledge of the spectrum of imaging findings of these infectious diseases, as well as the effect that treatment has on imaging appearances, is important in the evaluation of HIV-infected patients.

radiographics.rsnajnls.org

Abbreviations: ADC = apparent diffusion coefficient, AIDS = acquired immunodeficiency syndrome, CMV = cytomegalovirus, CNS = central nervous system, FLAIR = fluid-attenuated inversion recovery, HAART =highly active antiretroviral therapy, H-E = hematoxylin-eosin, HIV = human immunodeficiency virus, IRIS = immune reconstitution inflammatory syndrome, NAA = *N*-acetylaspartate, PML = progressive multifocal leukoencephalopathy

RadioGraphics 2008; 28:2033–2058 • **Published online** 10.1148/rg.287085135 • **Content Code:** NR

[1]From the Departments of Radiologic Pathology (A.B.S.) and Neuropathology (E.J.R.), Armed Forces Institute of Pathology, Washington, DC; Department of Radiology and Radiological Sciences, Uniformed Services University of the Health Sciences, 4301 Jones Bridge Rd, Bethesda, MD 20814 (A.B.S., J.G.S.); and Department of Pathology, George Washington University, Washington, DC (E.J.R.). Received May 12, 2008; revision requested June 6; revision received July 11; accepted July 11. All authors have no financial relationships to disclose. **Address correspondence to** A.B.S. (e-mail: *alsmith@usuhs.mil*).

Introduction

The human immunodeficiency virus (HIV) is a retrovirus that infects cells of the immune system and destroys or disrupts their function. In the more advanced stages of HIV infection, acquired immunodeficiency syndrome (AIDS) develops. According to the Joint United Nations Programme on HIV/AIDS, an estimated 39.5 million people were living with HIV infection at the end of 2006 (1). HIV is a neurotropic virus that enters the central nervous system (CNS) early in the course of infection (2,3). Up to 60% of AIDS patients will have neurologic manifestations, and, in the era before use of highly active antiretroviral therapy (HAART), neurologic disease was the first manifestation of symptomatic HIV infection in 10%–20% of patients (4,5). HIV crosses the intact blood-brain barrier, and the virus has been cultured from the brain, nerve, and cerebrospinal fluid of patients at all stages of disease (6,7). This virus infects the cells of the monocyte-macrophage lineage, and the indirect effects on macrophage activation are implicated as a cause of nervous system injury in HIV infection. Although HIV has previously been described as not directly infecting the astrocytes or oligodendrocytes, evidence is building that HIV may infect these cells as well (3,8,9).

Neurologic complications arise from the HIV infection itself, from secondary opportunistic infections and neoplasms, and from drug-related complications of therapy. The opportunistic infections are varied and include progressive multifocal leukoencephalopathy (PML), cytomegalovirus (CMV) infection, and fungal infections. A resurgence of CNS tuberculosis and neurosyphilis has also occurred with the advent of HIV infection. Development of neurologic manifestations depends on a variety of factors, including therapy with antiretroviral drugs and the patient's overall degree of immunosuppression. A decrease in the CD4 receptor–positive T lymphocytes is the best predictor of the potential development of opportunistic infections. The patient is most vulnerable when the CD4 count falls below 200 cells/μL (10). Neuroradiologic findings in HIV infection vary, depending on the underlying etiology. In addition, multiple conditions may involve the nervous system simultaneously.

The advent of HAART, which has been used in Western countries to treat HIV-infected patients since 1996, has resulted in a decline in the incidence of neurologic complications, especially those caused by opportunistic infections (11,12). In countries where HAART is available, cognitive dysfunction and peripheral neuropathies caused directly by HIV represent the majority of cases of HIV-related neurologic disorders; in other countries, opportunistic infections of the CNS are more common. Immune reconstitution inflammatory syndrome (IRIS) is a complication of HAART that causes transient worsening or appearance of new signs, symptoms, or radiologic manifestations of opportunistic infection after initiation of therapy. Occasionally, IRIS may be associated with a fatal outcome. IRIS is thought to arise from restoration of immune response, and it impacts the imaging findings.

Knowledge of the imaging findings associated with the various infectious agents that involve the CNS in HIV-infected patients, as well as the impact of treatment on them, is important in guiding therapy. In this article, we summarize the current literature as well as our own experience with HIV cases from the Radiologic Pathology Archives at the Armed Forces Institute of Pathology (AFIP). The clinical, pathologic, and imaging features of AIDS dementia complex, PML, toxoplasmosis, CMV infection, fungal infections, tuberculosis, and neurosyphilis are emphasized, followed by a brief discussion of IRIS.

AIDS Dementia Complex

AIDS dementia complex is an HIV-associated, chronic, neurodegenerative syndrome characterized by progressive cognitive and motor impairment and atrophic changes involving the brain. Although AIDS patients have improved survival rates because of antiretroviral therapy, approximately 15%–20% of these patients develop AIDS dementia complex, and it is one of the most common causes of morbidity in this group in the United States (12,13).

Epidemiology and Clinical Features

AIDS dementia complex occurs during the later stages of AIDS and predominantly affects the white matter by producing demyelination and gliosis (13,14). The diagnosis is based on the clinical findings of CNS neurologic dysfunction, which include inattention, indifference, and psychomotor slowing, and on objective measures of dysfunction that are based on standardized neuropsychologic tests. The neurologic dysfunction can further progress to frank dementia, and the viral load in the cerebrospinal fluid helps predict the increased risk

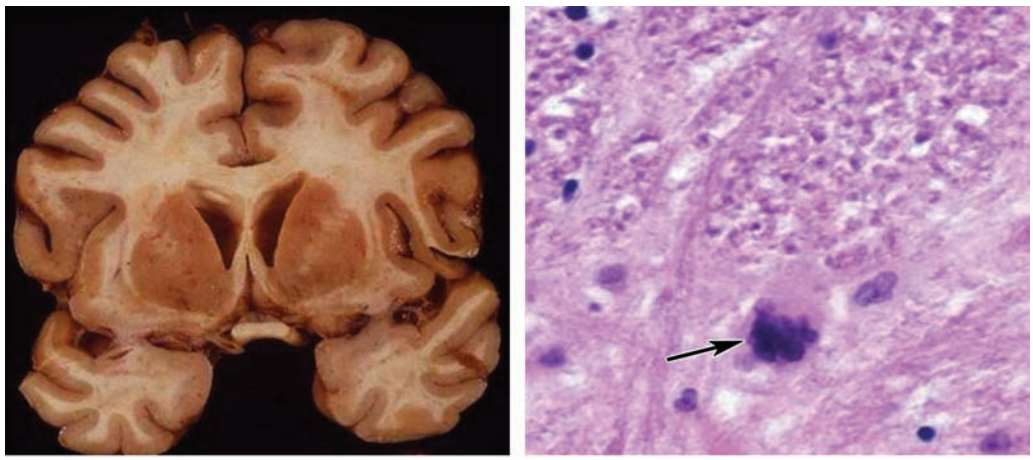

a. b.

Figure 1. AIDS dementia complex in a 27-year-old man. **(a)** Photograph of a gross specimen demonstrates that the sulci are prominent for the patient's age, consistent with a marked reduction in brain volume. **(b)** Photomicrograph (original magnification, ×200; hematoxylin-eosin [H-E] stain) shows a multinucleated giant cell (arrow), which is characteristic of HIV encephalitis.

for dementia (15). Patients with CD4 counts less than 200 cells/μL, longer duration of HIV infection, and older age at seroconversion are at most risk for developing AIDS dementia complex (16).

Pathologic Features

The underlying pathogenesis for AIDS dementia complex is still not fully understood. Studies of animal models suggest that meningeal inflammation occurs initially, along with an associated perivascular HIV-infected monocyte proliferation that disrupts the blood-brain barrier. HIV then gains direct access to the brain and infects the microglial cells (which are macrophages), thus resulting in their activation and proliferation. This process creates multinucleated giant cells and microglial nodules. The microglial cell activation also causes an inflammatory response that leads to injury of neural tissue (17–20). The severity of symptoms corresponds to the overall viral load within the CNS (15).

At gross inspection, the brain volume appears markedly reduced (ie, atrophic) compared with norms for the patient's age (Fig 1a). According to histopathologic analysis, patients either have HIV encephalitis, HIV leukoencephalopathy, or both; some authors consider these conditions to be the extremes of a spectrum of HIV-induced disease (21). In HIV encephalitis, pericapillary multinucleated giant cells are seen, along with myelin loss, reactive astrocytosis, and microglial activation with microglial nodules (Fig 1b). Diffuse myelin loss, astroglial proliferation, and infiltration by mono- and multinucleated macrophages characterize HIV leukoencephalopathy (21,22). Cortical and deep central gray matter is also involved with a diffuse reactive astrocytosis and microglial activation; neuronal loss may also be seen (23).

Imaging Features

The imaging findings of AIDS dementia complex are frequently referred to as HIV encephalitis. In patients with AIDS dementia complex, computed tomography (CT) shows diffuse, symmetric cerebral atrophy that is out of proportion for the patient's age. In addition, symmetric abnormal low attenuation in the periventricular and deep white matter is noted (Fig 2a). HIV encephalopathy does not result in mass effect or enhancement. If either of these findings is present, another diagnosis must be considered.

Teaching Point

On magnetic resonance (MR) images, a diffuse cerebral atrophy with symmetric, patchy or confluent areas of T1 and T2 prolongation are seen within the periventricular and deep white matter of patients with AIDS dementia complex. Often, there is a frontal predominance that may include involvement of the genu of the corpus callosum. Neither enhancement nor mass effect is observed (Fig 2b, 2c). Proton (^{1}H) MR spectroscopy reveals decreased *N*-acetylaspartate (NAA) and elevated peaks of in choline and myoinositol (24,25).

a.

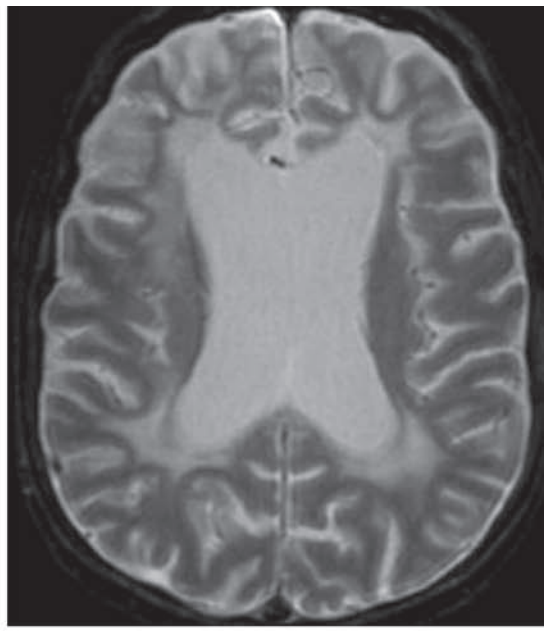

b.

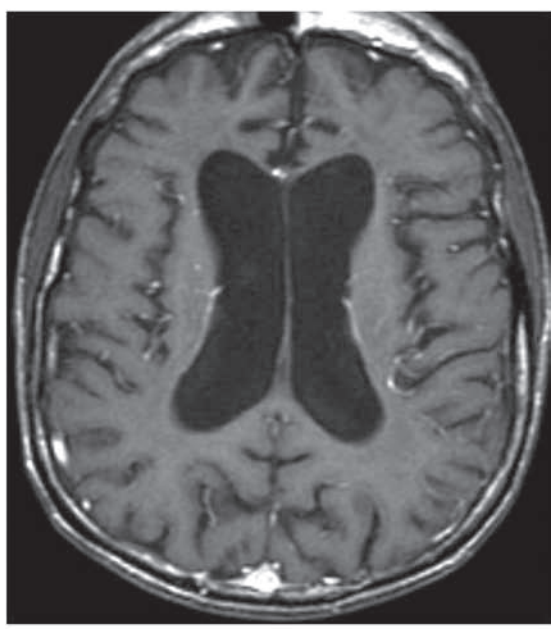

c.

Figure 2. AIDS dementia complex in a 36-year-old man with progressive dementia. **(a)** Unenhanced axial CT image demonstrates prominence of the sulci and ventricles, findings consistent global volume loss. Symmetric, low attenuation is present in the periventricular white matter. **(b)** Axial T2-weighted image demonstrates prominence of the sulci and ventricles, findings consistent with diffuse atrophy. Symmetric, periventricular hyperintensity corresponds to the regions of low attenuation seen on the CT image. There is no associated mass effect. **(c)** Postcontrast (ie, contrast material–enhanced) T1-weighted image shows that no enhancement is associated with the regions of T2 hyperintensity.

Thurnher et al (26) found that AIDS dementia complex patients treated with HAART demonstrated some improvement in abnormal signal intensity; however, the authors cautioned that in some patients the signal abnormalities worsen on initial follow-up and eventually improve over time. Diffusion tensor imaging depicts abnormalities in mean diffusivity and fractional anisotropy in the subcortical white matter, even when the white matter appears normal on conventional T1- and T2-weighted MR images (27,28).

Treatment and Prognosis

Before HAART was available, the median survival time of an AIDS dementia complex patient after the onset of dementia was 6 months (14,29). In an Australian study, a sevenfold improvement in survival was noted in patients with AIDS dementia complex treated with HAART (29). In their study, Dore et al (29) found that the number of people living with AIDS dementia complex had increased, but the number of new AIDS dementia complex cases had declined.

Progressive Multifocal Leukoencephalopathy

PML is a progressive demyelinating disorder that results from a viral infection of the myelin-producing oligodendrocytes. The infecting agent is the John Cunningham virus, which is a DNA papovavirus. The majority of patients with PML are believed to be infected with the John Cunningham virus in childhood or early adolescence; the virus remains latent in the CNS unless reactivated in the setting of immunodeficiency (30).

Epidemiology and Clinical Features

PML is found in approximately 5% of autopsies of patients who die of AIDS (31). The greatest risk of developing PML occurs among patients with CD4 counts in the range of 50–100 cells/μL. PML typically results in a progressive neurologic decline, and patients develop cognitive impairment, altered mental status, and personality changes. Motor and sensory changes also occur, and the patients may develop seizures. Without treatment, patients have a progressive downhill course, with death occurring within 1 year of diagnosis of PML in 90% of cases (32). Polymerase chain reaction testing of the cerebrospinal fluid for the John Cunningham virus assists in making the diagnosis, with a specificity approaching 96% (33,34). However, Marzocchetti et al (35) found that the sensitivity of polymerase chain reaction testing has decreased from 90% to 58% since the institution of HAART. The cause of this finding is not understood.

Pathologic Features

The John Cunningham virus directly infects the oligodendrocytes, which are then unable to maintain myelin, and denuded axons and focal areas of demyelination result (Fig 3a). Inflammatory reaction is usually blunted, a feature that accounts for the typical absence of mass effect and vasogenic edema. At gross inspection, the degree of brain atrophy is milder than that seen with AIDS dementia complex, and areas of demyelination and, occasionally, necrosis are seen. Frequently, these findings are found in the subcortical white matter (Fig 3b, 3c). Multiple lesions are common, but solitary lesions may be seen as well. Histopathologic analysis reveals astrocytes with bizarre, pleomorphic nuclei and enlarged oligodendrocyte nuclei with a ground-glass appearance and scanty perivascular inflammation (Fig 3d). At electron microscopy, virons are seen within the nuclei of oligodendrocytes, and viral particles may appear as filamentous or spherical forms, referred to as the "spaghetti and meatball" appearance (Fig 3e).

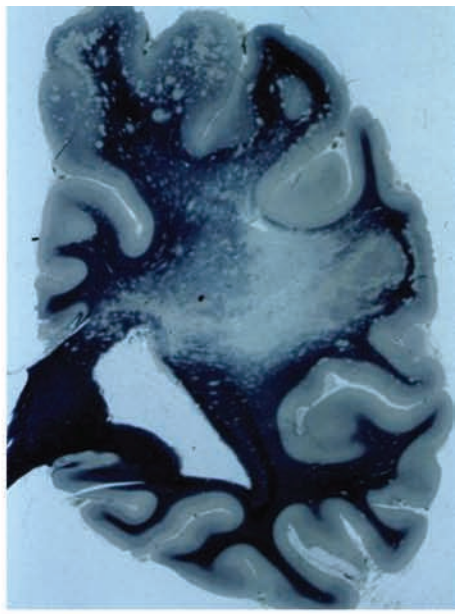

a.

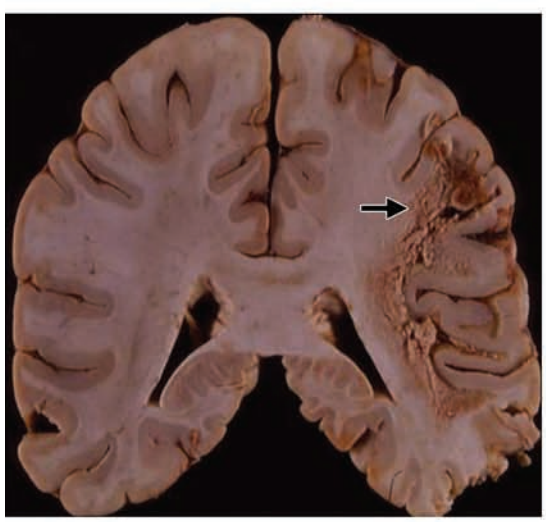

b.

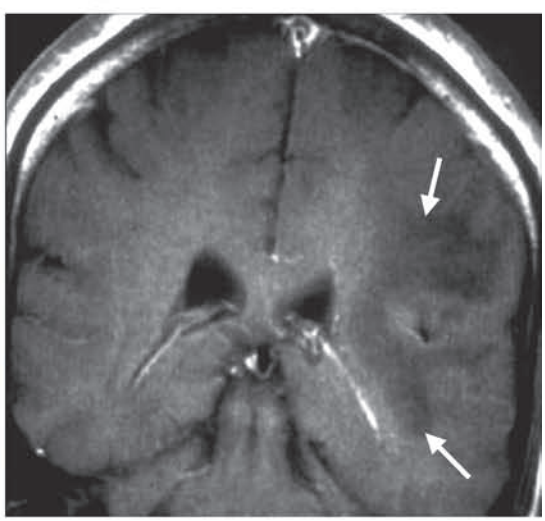

c.

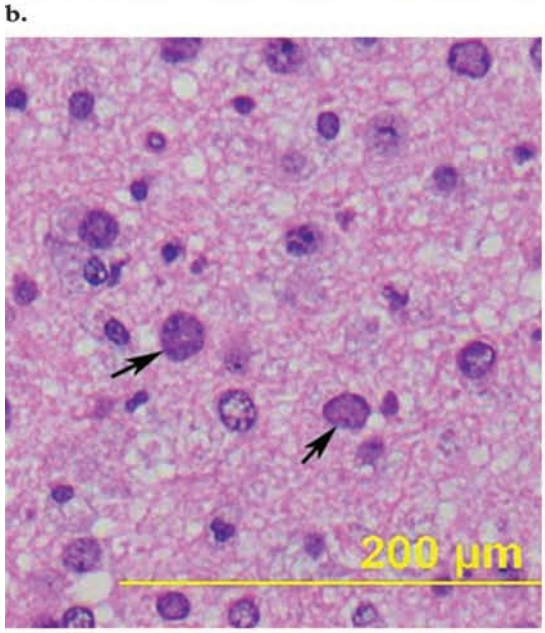

d.

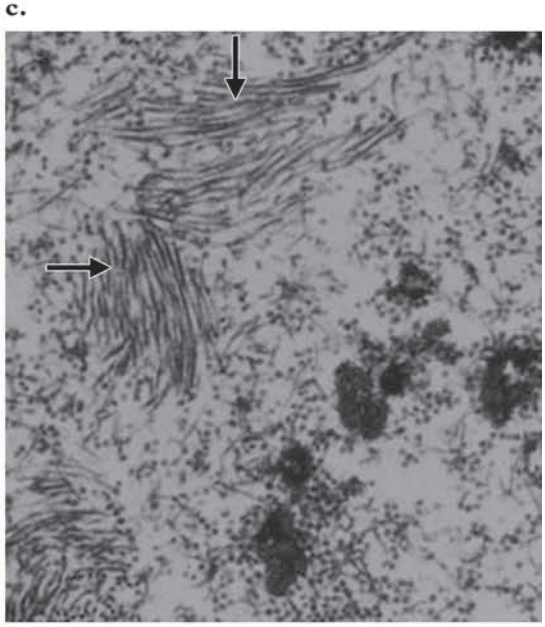

e.

Figure 3. PML in a 30-year-old man with AIDS. **(a)** Photograph of a specimen stained with myelin stain (blue) shows areas without stain, a finding consistent with demyelination. **(b)** Photograph of a gross specimen demonstrates areas of subcortical demyelination that appears to be grossly necrotic in some regions (arrow). **(c)** Coronal postcontrast T1-weighted image, corresponding to the gross specimen in **b**, shows low signal intensity (arrows) involving the white matter of the left hemisphere, including the subcortical U fibers. No enhancement is seen. **(d)** Photomicrograph (original magnification, ×200; H-E stain) demonstrates enlarged oligodendroglial nuclei with a ground-glass appearance (arrows) that are characteristic for PML. **(e)** Electron micrograph reveals viral particles within an oligodendrocyte nucleus that are both spherical and filamentous (arrows): the "spaghetti and meatball" appearance.

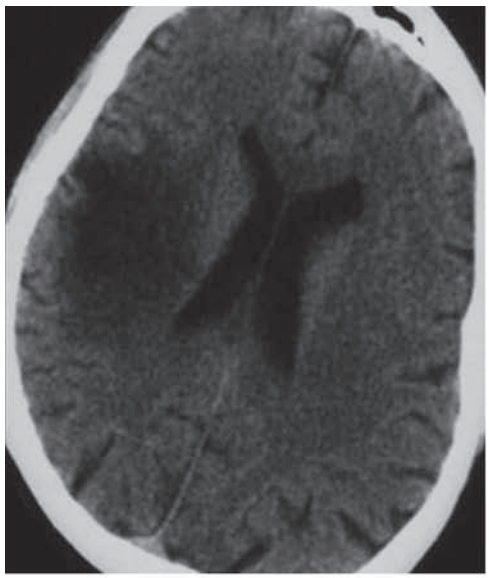

a.

b.

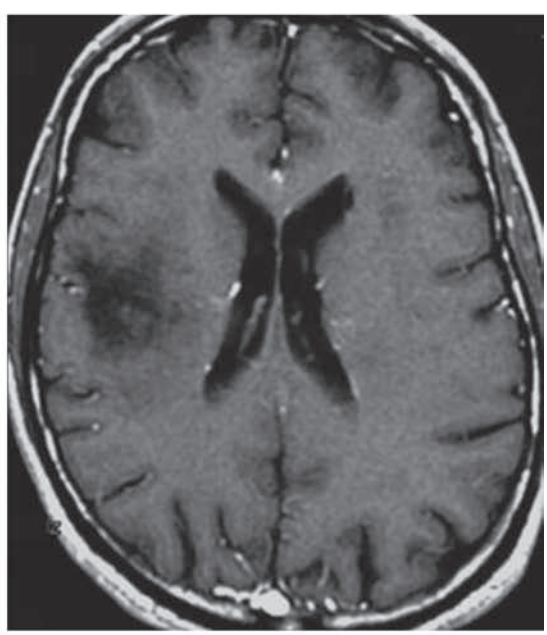

c.

Figure 4. PML in a 30-year-old woman with HIV infection. **(a)** Axial unenhanced CT image reveals a focal area of low attenuation within the white matter of the right hemisphere. The subcortical U fibers are involved, and no mass effect is present. **(b)** Axial T2-weighted image depicts hyperintensity involving the white matter of the right hemisphere, including the subcortical U fibers. No mass effect is seen. **(c)** Axial postcontrast T1-weighted image demonstrates hypointensity and no evidence of associated enhancement.

Imaging Features

Teaching Point

In patients with PML, CT reveals asymmetric focal zones of low attenuation that involve the periventricular and subcortical white matter (Fig 4a). This appearance is a differential diagnostic feature compared with the typically more symmetric areas of low attention seen in patients with HIV encephalopathy. On MR images, there are typically multifocal, asymmetric areas of T1 and T2 prolongation in the periventricular and subcortical white matter (Fig 4b, 4c). These lesions are frequently bilateral and multiple, although they may occasionally be solitary. Subcortical U fiber involvement is frequently seen, a finding that provides a sharp contrast with the overlying gray matter. Mass effect and hemorrhage are unusual, but, if present, they are typically mild (36–38). Typically, PML lesions do not enhance, but faint peripheral enhancement has been described (Fig 5). Results reported in a few studies suggest that enhancement is associated with an improved survival rate (32,39). In one study, 50% of the long-term survivors had enhancement of PML lesions at MR imaging, compared with only 8.9% of the short-term survivors (32). In these cases, the enhancement was described as faint and peripheral (32). Enhancement has been proposed to be related

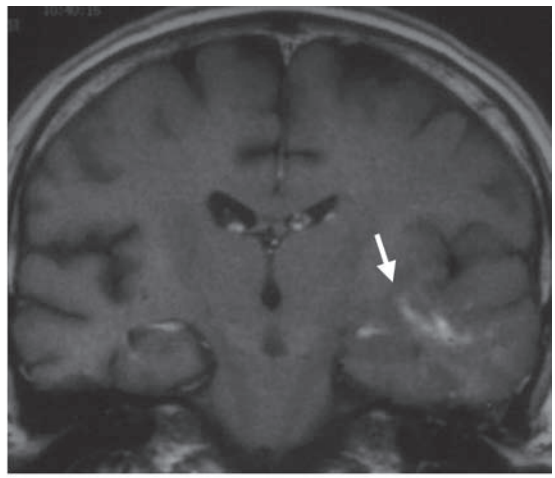

a.

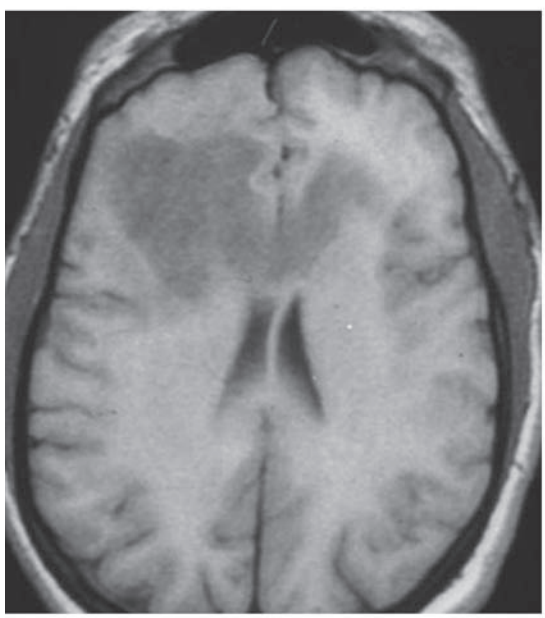

b.

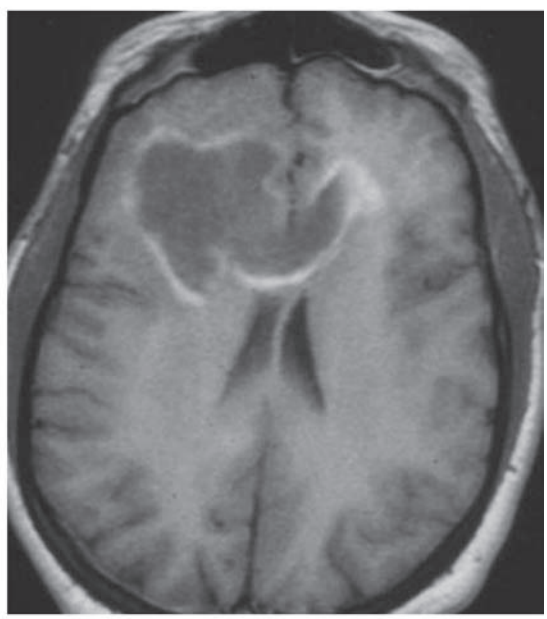

c.

Figure 5. **(a)** PML in a 30-year-old woman with HIV infection. Coronal postcontrast T1-weighted image shows patchy enhancement (arrow) in the left temporal lobe. **(b, c)** PML in a 25-year-old man with AIDS. **(b)** Axial T1-weighted image demonstrates an area of low signal intensity involving the white matter of the right frontal lobe that crosses the corpus callosum to the white matter of the left frontal lobe. Mild mass effect is present. **(c)** Axial postcontrast T1-weighted image demonstrates peripheral enhancement, which is more confluent than typically seen in patients with PML. A neoplastic process, such as lymphoma or glioma, would be in the differential diagnosis. At autopsy, the lesion proved to be PML.

to the patient's ability to mount an inflammatory response; however, in a study of radiologic-pathologic correlation, Whiteman et al (36) found no correlation between enhancement at MR imaging and inflammation seen in pathologic specimens (36). Others suggest that the enhancement results from immune response to viral antigen (40). When patients receive HAART, increased enhancement and mass effect have been reported, and these findings may be a result of IRIS if they are observed in the weeks following the initiation of therapy (26,41).

Evaluation of diffusion-weighted imaging in patients with PML has been limited. Apparent diffusion coefficient (ADC) values have been reported to be much higher in the center of a lesion than at its periphery, and some authors have described observation of a leading edge of high signal intensity on diffusion-weighted images (Fig 6) (41,42). Recent studies suggest that diffusion-weighted imaging may be useful for documenting response of PML to HAART. Usiskin et al (43) obtained serial ADC measurements by using a b value of 3000 sec/mm^{-2}, and they found a marked reduction of lesional ADC and a reconstitution of anisotropy in the affected areas that correlated with treatment response.

MR spectroscopy demonstrates a reduction in NAA, presence of lactate, and increased amounts of choline and lipids.

Toxoplasmosis

Toxoplasmosis, the most common mass lesion in patients with AIDS, is caused by the ubiquitous parasite, *Toxoplasma gondii* (44,45). It is an obligate intracellular protozoan that exists in three forms: oocysts, tachyzoites, and bradyzoites.

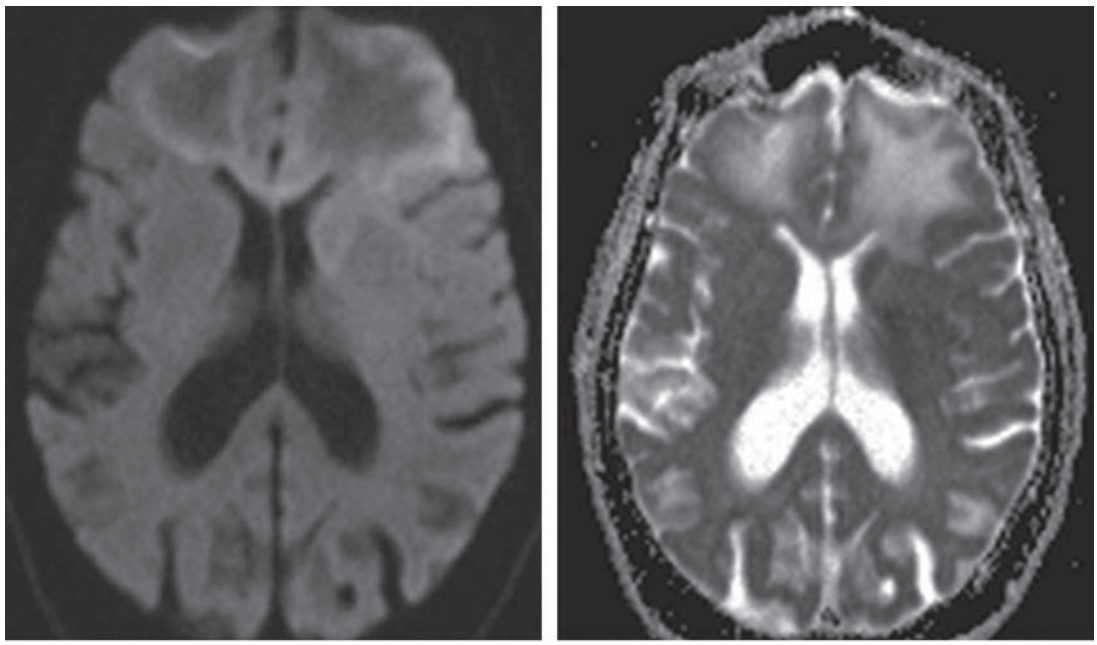

a. b.

Figure 6. PML in a 28-year-old woman. **(a)** Diffusion-weighted image (b = 1000 sec/mm^{-2}) demonstrates hyperintensity along the periphery of a PML lesion that involves both frontal lobes. **(b)** ADC map demonstrates low signal intensity along the periphery and increased signal intensity centrally within the lesion.

Oocytes occur in the definitive hosts (members of the family Felidae) and infect humans when the organisms are inadvertently ingested. Tachyzoites are the rapidly multiplying form, and, when they localize to the CNS (or muscle), they convert to tissue cysts, known as bradyzoites.

Epidemiology and Clinical Features

Cerebral toxoplasmosis, the most common opportunistic CNS infection in AIDS patients, occurs in 15%–50% of cases (46). With the introduction of HAART, the number of cases has declined (47). A total of 20%–70% of the entire population of the United States demonstrates seropositivity for *T gondii*, and, in most cases, cerebral toxoplasmosis results from a reactivation of a latent infection (48). Therefore, a positive antibody titer is not diagnostic of active toxoplasmosis. However, a negative titer is not helpful because up to 20% of patients with AIDS may not have detectable antitoxoplasma antibodies (49). Polymerase chain reaction testing of peripheral blood samples has sensitivity and specificity for the diagnosis of cerebral toxoplasmosis as high as 80% and 90%, respectively (50). Polymerase chain reaction testing of cerebral spinal fluid has a variable sensitivity, with results ranging from 11.5% to 100%, but its specificity is high (96%–100%) (50). HIV-infected patients become most susceptible to developing active toxoplasmosis when their CD4 counts reach less than 100 cells/μL. Patients may present with symptoms from mass effect, focal neurologic deficits, seizures, or cranial nerve palsies.

Pathologic Features

Toxoplasmosis typically results in necrotizing encephalitis, although rare nonnecrotizing examples are associated with microglial nodules and astrogliosis (Fig 7a). Intra- and extracellular *Toxoplasma* tachyzoites are numerous. Cysts containing bradyzoites are usually found at the periphery of necrotic areas (Fig 7b). The regions of the corticomedullary junction, basal ganglia, and thalamus are affected most often; however, the brainstem may also be involved.

Imaging Features

Unenhanced CT reveals multiple areas of abnormal low attenuation that appear most frequently in the basal ganglia, thalamus, and corticomedullary junction (51). These areas demonstrate ring or nodular enhancement on postcontrast CT images.

At MR imaging with T2-weighted sequences, toxoplasmosis lesions are typically hypo- to isointense and are surrounded by high-signal-intensity vasogenic edema (Fig 7b). Hemorrhage may be seen occasionally, a finding that can help differentiate toxoplasmosis from lymphoma, which typically does not hemorrhage before treatment (52). Postcontrast MR imaging reveals multiple nodular lesions or ring-enhancing lesions (Fig 7c). Occasionally, a small eccentric nodule

Teaching Point

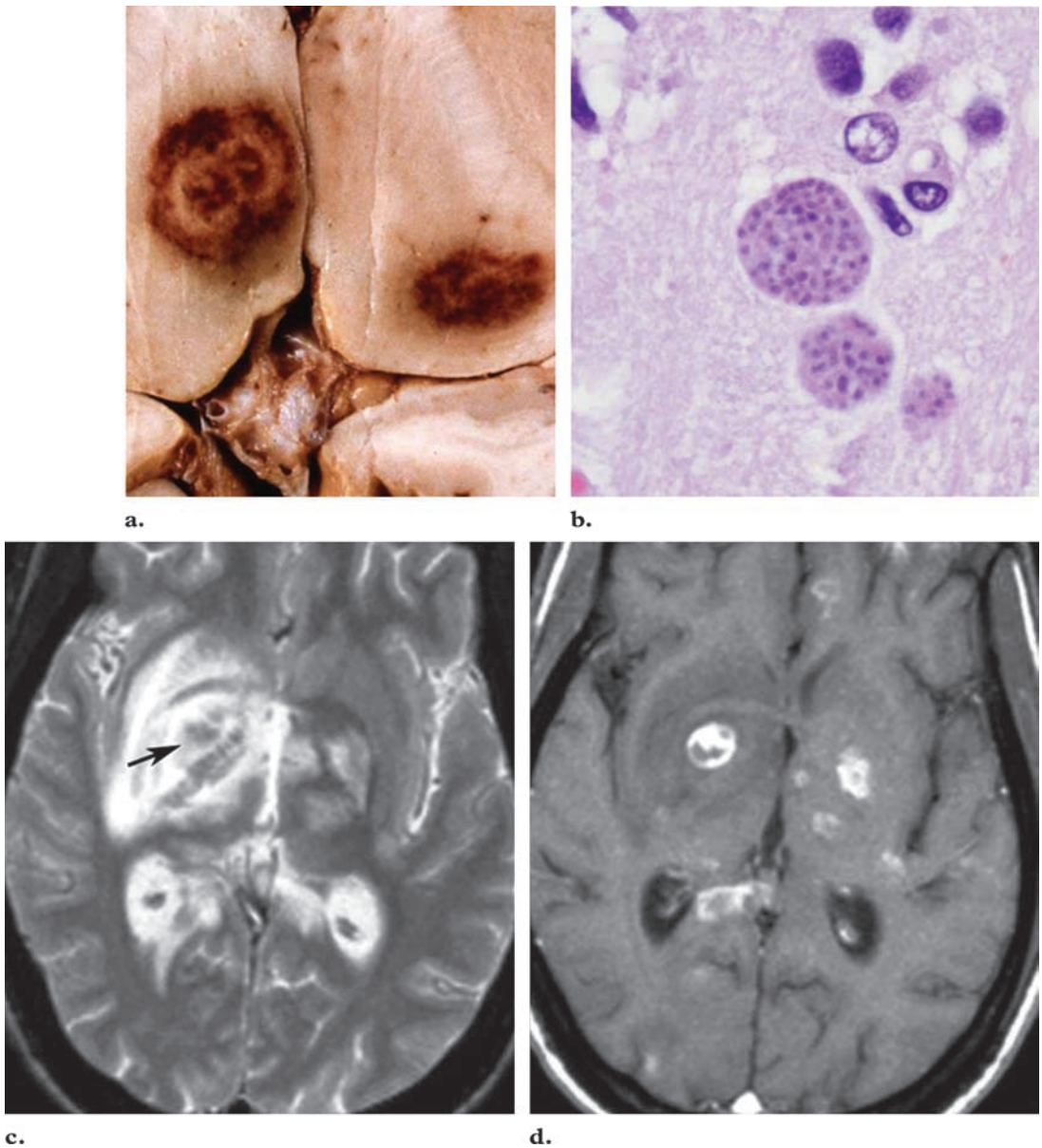

Figure 7. Toxoplasmosis in a 28-year-old man with HIV infection. **(a)** Photograph of a gross specimen shows necrotic-appearing mass lesions in the bilateral basal ganglia. **(b)** Photomicrograph (original magnification, ×200; H-E stain) demonstrates cysts that contain bradyzoites. **(c)** Axial T2-weighted image demonstrates a region involving the right basal ganglia that is isointense to hypointense relative to gray matter (arrow). The lesion is surrounded by high-signal-intensity vasogenic edema. Smaller lesions are present in the left basal ganglia. **(d)** Axial postcontrast T1-weighted image demonstrates multiple enhancing lesions.

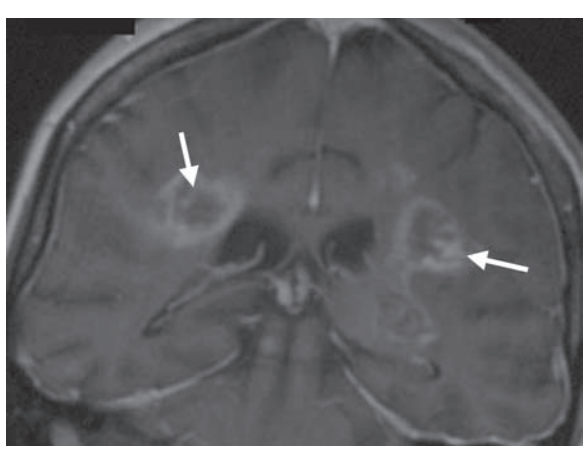

Figure 8. Toxoplasmosis in a 31-year-old patient with AIDS who presented with headaches and altered mental status. Coronal postcontrast T1-weighted image demonstrates ring-enhancing lesions with eccentric nodules: the "target sign" (arrows). Mild, linear dural enhancement was presumed to be from a recent lumbar puncture.

Figure 9. Acute toxoplasmosis in a 37-year-old man with a previous history of toxoplasmosis who had discontinued his prophylactic therapy. **(a)** Axial unenhanced CT image reveals a peripherally calcified lesion (arrow) in the right caudate head that is a sequela of previous toxoplasmosis infection. The low-attenuation mass lesion with surrounding vasogenic edema in the region of the left basal ganglia is from a new focus of toxoplasmosis. **(b)** Axial FLAIR (fluid-attenuated inversion recovery) image demonstrates marked vasogenic edema that involves the region of the left basal ganglia and thalamus and that surrounds a region of low signal intensity. Low signal intensity secondary to calcification is seen around the lesion in the region of the right caudate head. **(c)** Spectrum from ^{1}H MR spectroscopy from the region of the low-signal-intensity lesion seen in **b** demonstrates a markedly elevated lipid-lactate peak (bracket). Small amounts of choline and NAA are also seen because of volume averaging with the surrounding brain tissue. (Case courtesy of Max Wintermark, MD, University of California, San Francisco.)

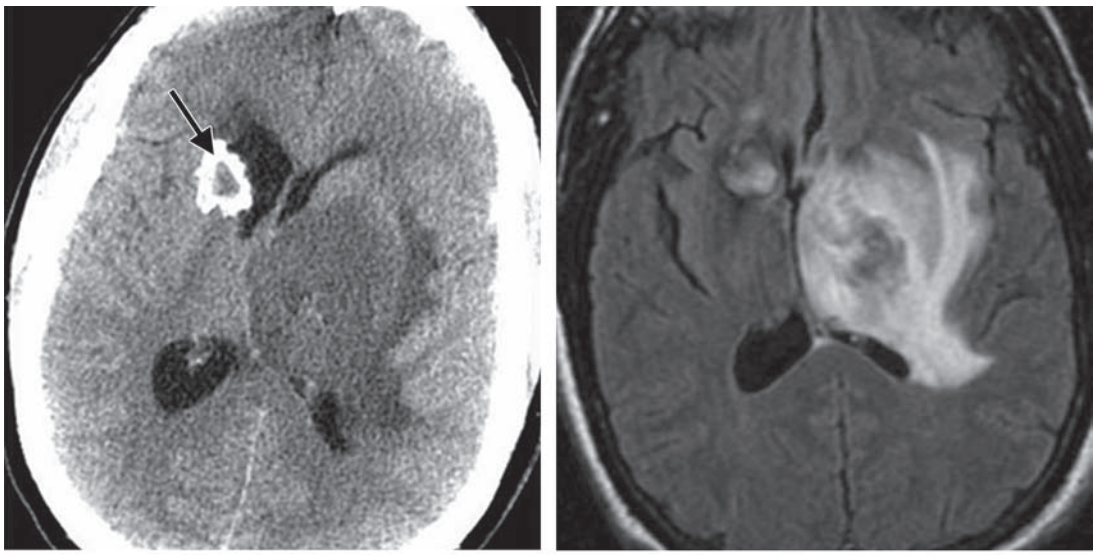

a. b.

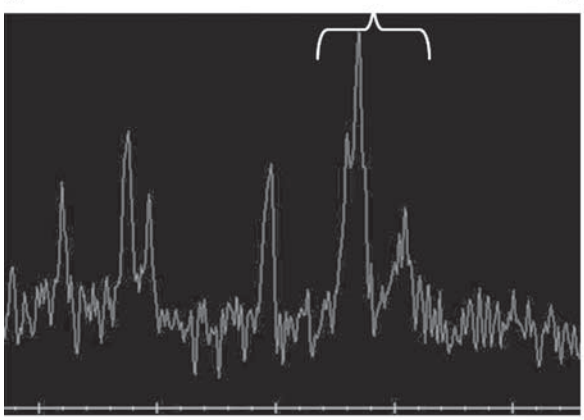

c.

rests alongside an enhancing ring: the "target sign" (Fig 8). This finding is highly suggestive of toxoplasmosis; however, it is relatively insensitive and is seen in less than 30% of cases (53). Toxoplasmosis occasionally involves the corpus callosum and may mimic a glioblastoma multiforme (54). Lesions from toxoplasmosis are usually multiple, and only in approximately 14% of cases are they solitary (55).

Differential Diagnosis

Patients with the "typical" imaging findings of toxoplasmosis are usually treated empirically for the disease. However, because lymphoma and toxoplasmosis can have very similar imaging appearances, follow-up evaluation is mandatory. After adequate treatment—a multidrug regimen of pyrimethamine sulfadiazine, and folic acid—the number and size of the lesions as well as their associated mass effect should decrease. This reduction may take anywhere from 2 to 4 weeks and up to 6 months. At sites of previous disease, the brain may appear normal or there may be encephalomalacia or calcification (Fig 9a, 9b). All lesions need to be followed to resolution, since multiple pathologic conditions may coexist in immunocompromised patients.

When considerable improvement after treatment does not appear, performance of thallium-201 brain single photon emission computed tomography (SPECT), fluorodeoxyglucose

positron emission tomography (FDG PET), or MR spectroscopy may be useful for reevaluation of the patient. Lymphoma lesions will result in positive findings at SPECT and FDG PET, and toxoplasmosis will not; however, lymphoma lesions smaller than 2 cm may result in negative findings. In addition, the reported sensitivities of these two imaging modalities have been variable (56–58). At ^{1}H MR spectroscopy, lymphoma demonstrates elevated peaks of choline, and MR perfusion typically shows an elevated relative cerebral blood volume in lymphoma but not in toxoplasmosis. Toxoplasmosis demonstrates elevated peaks of lipid and lactate, findings that, unfortunately, can also be seen in lymphoma if the voxel is placed over the necrotic, rather than cellular portion, of the lesion (59,60). Decreased peaks of NAA and moderately decreased peaks of choline have also been reported (61) (Fig 9c). If a patient is receiving steroids, it will be impossible to assess lesion activity accurately because steroids reduce the degree of enhancement and diminish associated edema and mass effect. Diffusion-weighted imaging has been suggested to help differentiate between the two diseases, as lymphoma typically has reduced diffusion. Unfortunately, toxoplasmosis demonstrates a wide range of diffusion characteristics, which can overlap with those of lymphoma (62).

Differentiating lymphoma from toxoplasmosis may be difficult with imaging findings alone, because both entities may produce focal, enhancing mass lesions and both are common in AIDS patients. Toxoplasmosis abscesses have been described as being smaller and more numerous. In addition, if a periventricular pattern is present, this finding suggests lymphoma, since toxoplasmosis uncommonly involves the ependyma.

Treatment and Prognosis

Toxoplasmosis will recur if therapy is discontinued. Treatment is effective against the free tachyzoites but not the encysted forms; thus, patients require lifelong maintenance therapy.

CMV Infection

CMV is a very common herpes virus that does not produce clinical disease in most people with an intact immune system.

Epidemiology and Clinical Features

CMV remains in latent form in the general population and reactivates in the setting of immune suppression. CNS involvement typically assumes the form of meningoencephalitis or ventriculitis, but it can also take the form of myelitis, polyradiculitis, and retinitis. Patients who develop CMV retinitis have a tenfold increased risk of developing CMV encephalitis. CMV may also cause a rapidly ascending polyneuropathy. A clinical diagnosis of CMV infection occurs in less than 2% of AIDS patients with neurologic disorders; however, at autopsy, evidence of CMV is found in 10%–40% of patients (63). CMV infection usually occurs when the CD4+ count falls below 50 cells/μL. The introduction of HAART resulted in a decreased prevalence of CMV infection and increased survival in AIDS patients.

Pathologic Features

Histologic identification of characteristic eosinophilic intranuclear inclusions surrounded by halos confirms the diagnosis of CMV infection. Microglial nodular encephalitis and ventriculoencephalitis are the most common histopathologic patterns (63).

Imaging Features

Imaging findings of CNS involvement in patients with CMV infection are frequently nonspecific, and, in most cases, findings from CT and MR imaging are normal. Demyelination can result in diffuse white matter abnormalities that appear as areas of low attenuation on CT images and of hyperintensity on T2-weighted MR images. CMV infection may also produce a suggestive, if not characteristic, pattern of ependymitis. In CMV meningoencephalitis or ventriculitis, low attenuation may be seen in the white matter, and ependymal enhancement may be seen on contrast-enhanced CT images. T2-weighted MR images demonstrate focal or diffuse increased signal intensity in white matter, as well as ependymal, subependymal, and periventricular T2 hyperintensity (Fig 10). In rare cases, CNS involvement with CMV may manifest as a ring-enhancing or space-occupying lesion.

Differential Diagnosis

The differential diagnosis of CMV ventriculitis includes bacterial ventriculitis; however, patients with the latter infection are typically acutely ill, a clinical finding that aids diagnosis. Lymphoma can also result in ependymal enhancement; however, it is more often nodular and irregular.

Treatment and Prognosis

CMV ventriculitis may result in death days to weeks after the onset of clinical symptoms. In cases of CMV encephalopathy, treatment with gangcyclovir and foscarnet may improve the patient's neurologic status, although the improvement may be short-lived.

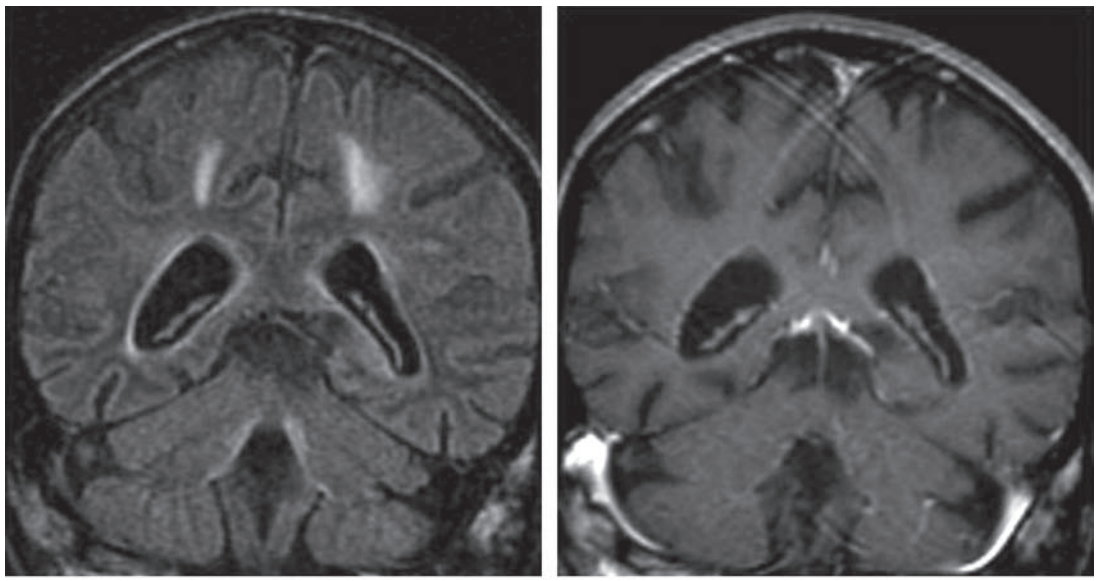

a. b.

Figure 10. CMV ependymitis in a 30-year-old man with AIDS. **(a)** Coronal T2-weighted FLAIR image demonstrates circumferential hyperintensity surrounding the lateral and fourth ventricles. Nonspecific T2 signal is present in the white matter. **(b)** Coronal postcontrast T1-weighted image reveals thin, linear periventricular enhancement. The nonspecific T2 hyperintensity in the white matter did not enhance. (Case courtesy of Max Wintermark, MD, University of California, San Francisco.)

Fungal Infection

Fungal infections are life threatening when they occur in the immunocompromised patient. The numbers of deaths from fungi in the immunocompromised population increased by fourfold in the past 20 years (64). The most commonly encountered fungi within this population are *Candida*, *Cryptococcus*, and *Aspergillus* species (65,66).

Cryptococcal Infection

Cryptococcus neoformans is an encapsulated, ubiquitous yeastlike fungus found in soil contaminated by bird excreta. Infection with *C neoformans* is the most common fungal infection of the CNS (4,67).

Epidemiology and Clinical Features.—*Cryptococcus* is the third most common cause of CNS infection in AIDS patients, ranking behind HIV and *Toxoplasma*. Before HAART, cryptococcal infection of the CNS occurred in up to 10% of patients, usually when the CD4 count dropped below 100 cells/μL (68–70). Cryptococcosis most likely spreads to the CNS by means of hematogenous dissemination from a pulmonary focus; however, reactivation of a latent cryptococcal infection is also possible (70,71). Symptoms are often nonspecific. Patients may present with signs of meningitis or, less frequently, meningoencephalitis. The detection of cryptococcal capsular polysaccharide antigen in the serum and cerebrospinal fluid aids in making the diagnosis.

Pathologic Features.—The main forms of cryptococcal infection are meningitis, pseudocysts, and cryptococcomas. At gross inspection, meningitis is seen as thickening and opacification of the leptomeninges. The pseudocysts are most frequent in the basal ganglia, and they have a "soap bubble" appearance, which is caused by the capsular material produced by the yeast (Fig 11a). Cryptococcomas are histologically characterized either as a chronic granulomatous reaction with fewer organisms or as lesions that contain numerous organisms and that are associated with mild inflammation. Lymphocytes, macrophages, and foreign body–type giant cells are typically seen. A collection of budding yeastlike cells within a gelatinous mass characterize the pseudocyst (Fig 11b). India ink and mucicamine are stains used to detect the organisms.

Imaging Features.—The radiologic manifestations of cryptococcosis are varied and frequently minimal. The imaging findings may consist of meningoencephalitis, intraventricular or intraparenchymal cryptococcomas, gelatinous pseudocysts, or hydrocephalus. Hydrocephalus, communicating or noncommunicating, is the most frequent, although nonspecific, finding of cryptococcal infection (72). *Cryptococcus* may spread along the perivascular spaces from the basilar cisterns, and cryptococcal infection may appear on images as rapidly growing, nonenhancing "cysts." Dilated perivascular spaces resulting from the presence of gelatinous pseudocysts are a frequent finding, and their presence in an immunocompromised patient should raise a red flag (Fig 11c).

Teaching Point

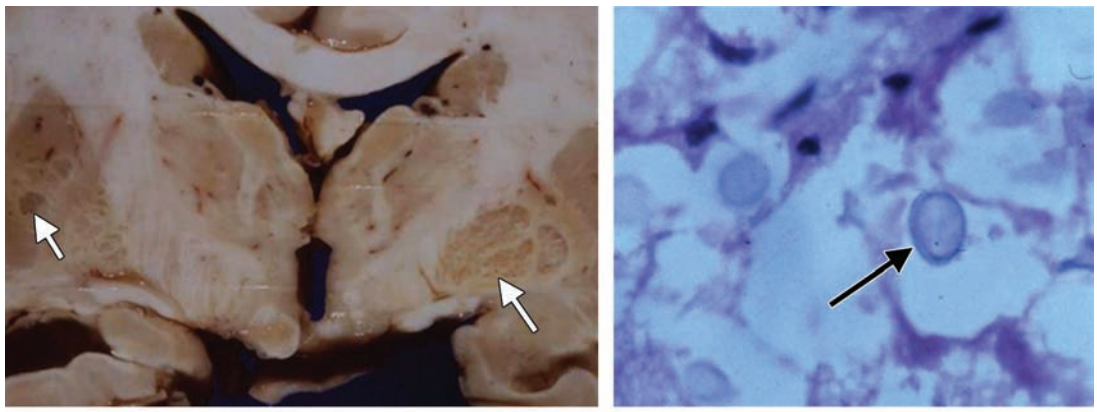

a. b.

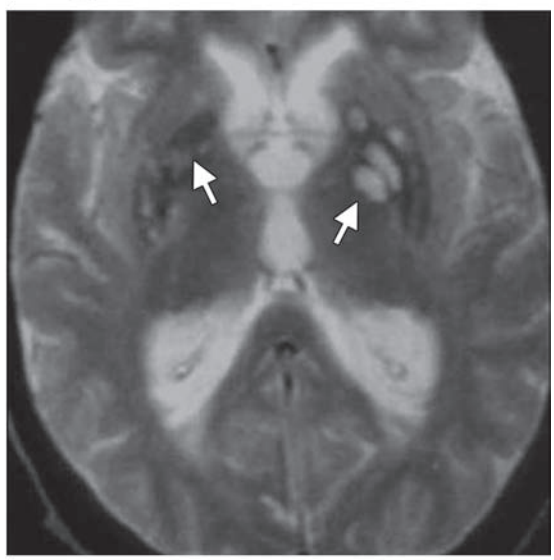

c.

Figure 11. Cryptococcal meningoencephalitis in a 42-year-old man with AIDS who became progressively obtunded. **(a)** Photograph of a gross specimen of the basal ganglia demonstrates lesions that have a soap bubble appearance (arrows). **(b)** Photomicrograph (original magnification, ×200; H-E stain) depicts faintly staining yeast (arrow). **(c)** Axial T2-weighted image shows multiple foci of high signal intensity within the bilateral basal ganglia, findings consistent with gelatinous pseudocysts in dilated perivascular spaces (arrows). Enlargement of the ventricles, consistent with hydrocephalus, is also present.

On CT images, cryptococcal lesions may have high or low attenuation; on MR images, they demonstrate T1 and T2 prolongation. Enhancement varies, but it is more likely to occur in immunocompetent hosts, since they can mount an effective inflammatory response. Cryptococcal lesions do not have reduced diffusion at diffusion-weighted imaging, a finding that may help distinguish them from pyogenic abscesses (73). Meningoencephalitis results in T2 hyperintensity within the region of involvement, and meningeal enhancement may be seen (Fig 12). Cryptococcomas within the brain parenchyma are rare (Fig 13) (73,74). Their appearance varies, but they may demonstrate surrounding vasogenic edema as well as nodular enhancement that results from compromise of the blood-brain barrier. The most common sites for cryptococcomas are the basal ganglia, thalamus, and cerebellum (75).

Differential Diagnosis.—The main differential diagnoses for an enhancing lesion in the basal ganglia are cryptococcoma, lymphoma, toxoplasmosis, and, to a lesser extent, pyogenic abscess. It is not possible to differentiate a cryptococcoma from a pyogenic abscess on conventional MR images. Subependymal lesions may appear similar

Figures 12, 13. **(12)** Cryptococcal meningoencephalitis in a 42-year-old woman. **(a)** Axial T2-weighted image demonstrates high signal intensity in the right occipital lobe. In addition, foci of hyperintensity are present in the bilateral basal ganglia (arrows), findings consistent with gelatinous pseudocysts. **(b)** Axial T1-weighted image demonstrates low signal intensity in the right occipital lobe that corresponds to the area of hyperintensity seen in **a**. **(c)** Axial postcontrast T1-weighted image demonstrates leptomeningeal enhancement in the region of the T2 hyperintensity. **(13)** Cryptococcoma in a 25-year-old HIV-infected patient who presented with increasing headache, nausea, and vomiting. **(a)** Axial T1-weighted image demonstrates a low-signal-intensity mass lesion in the right cerebellum. **(b)** On an axial T2-weighted image, the mass is heterogeneous in signal intensity but predominantly hyperintense, with a surrounding rim of T2 hyperintensity, a finding consistent with edema. **(c)** Axial postcontrast T1-weighted image reveals peripheral nodular enhancement of the lesion.

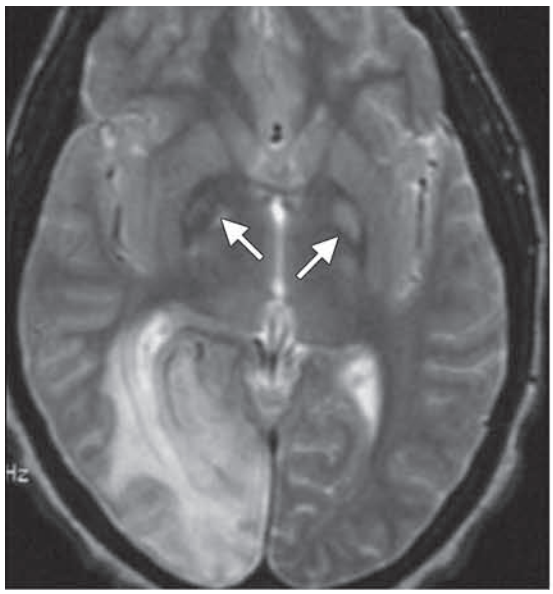

12a.

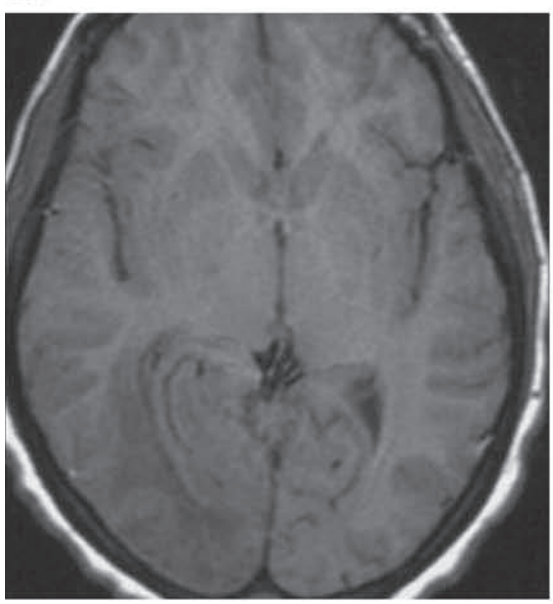

12b.

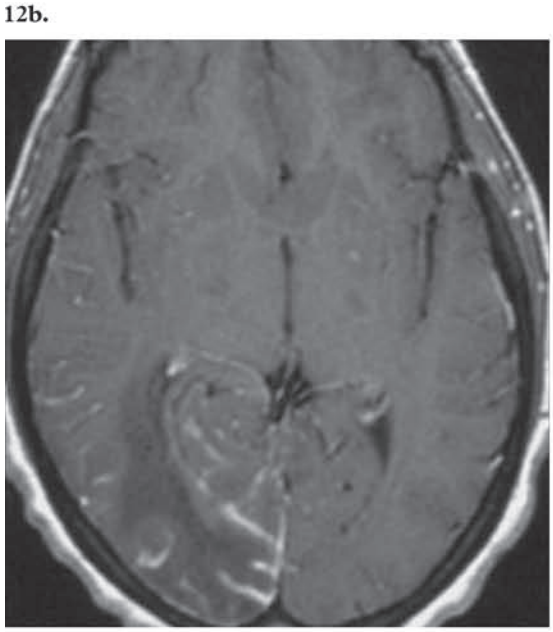

12c.

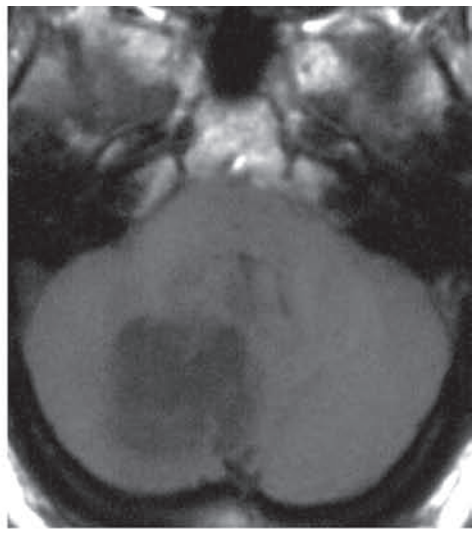

13a.

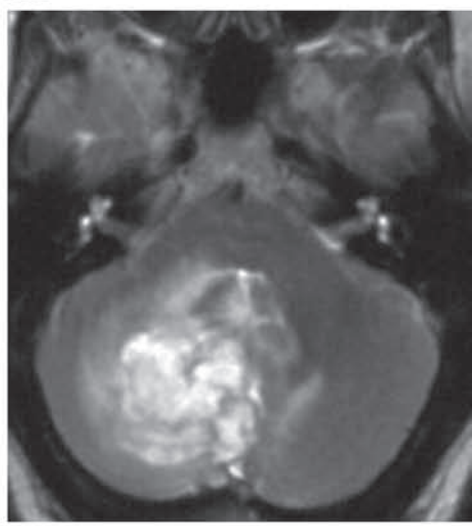

13b.

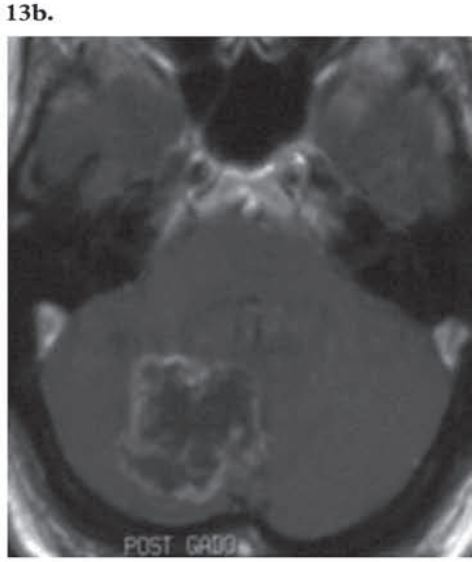

13c.

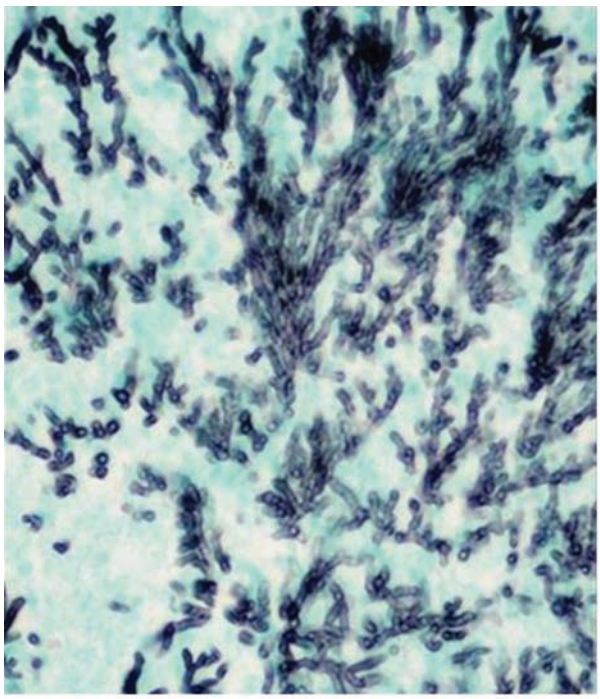

a.

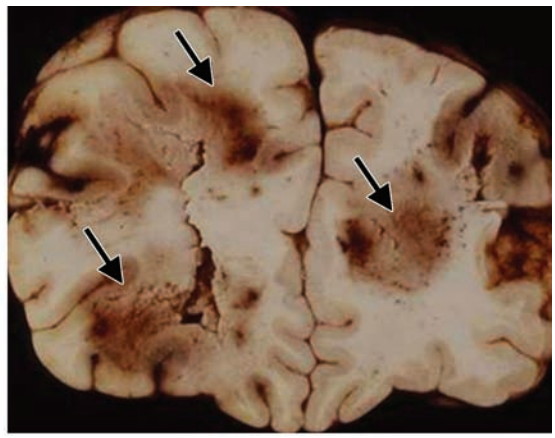

b.

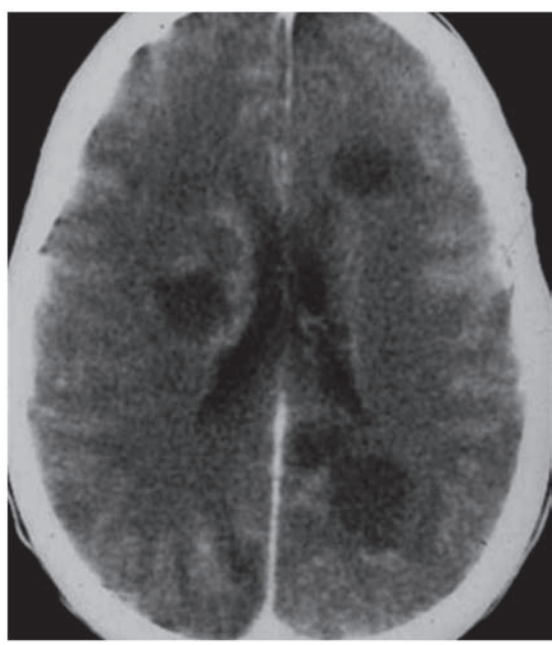

c.

Figure 14. Disseminated aspergillosis in a 38-year-old man with HIV infection. **(a)** Photomicrograph (original magnification, ×200; Grocott methenamine silver stain) reveals septate hyphae that branch at acute angles, an appearance consistent with *Aspergillus*. **(b)** Photograph of the gross specimen demonstrates several abscesses (arrows) with hemorrhagic foci. **(c)** Axial postcontrast CT image demonstrates multiple circumscribed regions of hypoattenuation with faint peripheral enhancement.

to lymphoma or CMV infection. Intraventricular cryptococcomas occasionally mimic racemose cysticercosis (76).

Treatment and Prognosis.—Cryptococcomas and pseudocysts frequently demonstrate improvement following treatment with antifungal agents such as fluconazole or amphotericin B. A mortality rate of 10%–30% occurs among patients treated for CNS meningoencephalitis, but without treatment the infection is uniformly fatal (77). Complications include hydrocephalus, seizures, dementia, and motor and sensory deficits.

Aspergillosis

Aspergillus species are septate hyaline molds that are ubiquitous throughout the world. They are found in soil, plants, and decaying matter. They are angioinvasive, and *A fumigatus* is the most common causative agent of aspergillosis.

Epidemiology and Clinical Features.—As with most fungal infections of the CNS in immunocompromised patients, cerebral involvement by *Aspergillus* results from hematogenous spread from a pulmonary focus, or the fungus may also directly invade the brain via the sinus. A resultant infectious vasculopathy may cause acute infarction or hemorrhage, or the fungus can extend into the surrounding tissue, resulting in an infectious cerebritis or abscess. *Aspergillus* has a predisposition to infect the perforating arteries. Involvement of the skull base and orbit leads to visual disturbance and cranial nerve palsies, and invasive sinonasal infections are lethal in greater than 50% of cases.

Pathologic Features.—*Aspergillus* species have septate hyphae that branch at acute angles (Fig 14a). They tend to invade blood vessels and

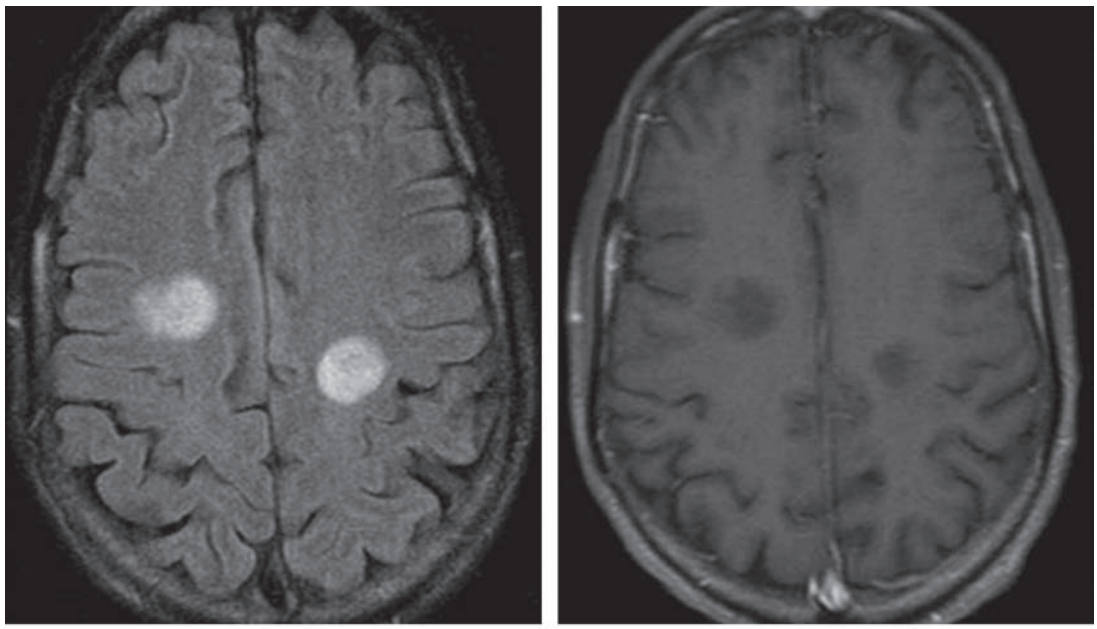

a. b.

Figure 15. Disseminated aspergillosis in a 39-year-old AIDS patient. **(a)** Axial T2-weighted FLAIR image shows two well-circumscribed foci of hyperintensity within the centrum semiovale. There is no significant surrounding edema. **(b)** Axial postcontrast T1-weighted image demonstrates low-signal-intensity lesions that do not demonstrate enhancement.

Figure 16. Aspergillosis in an HIV-infected patient who presented with rapidly progressive proptosis. Axial postcontrast T1-weighted image shows a peripherally enhancing low-signal-intensity mass within the left orbit that is causing proptosis. Intracranial extension is present, as evidenced by dural enhancement in the middle cranial fossa (arrow). Opacification and enhancement of the left ethmoid air cells is seen. In addition, enhancement is seen within the periorbital soft tissue and in the left temporalis muscle. (Courtesy of Max Wintermark, MD, University of California, San Francisco.)

spread along the internal elastica and lamina, resulting in vascular thrombosis and hemorrhagic infarcts with variable inflammation (Fig 14b). Typically, dissemination leads to multiple intraparenchymal lesions, often in the distribution of the middle cerebral artery.

Imaging Features.—Ashdown et al (78) described three imaging patterns for cerebral aspergillosis: *(a)* multiple cortical and subcortical regions of low attenuation on CT images, with T2 hyperintensity seen in corresponding areas on MR images (Fig 15); *(b)* multiple ring-enhancing lesions (Fig 14c); and *(c)* dural enhancement adjacent to enhancing lesions of the paranasal sinuses or calvaria (Fig 16). The presence of hemorrhage associated with the lesions and intraparenchymal hemorrhage in an immunocompromised patient should cause one to consider the possibility of aspergillosis (Fig 17). The ring enhancement may be subtle or well defined, which may be related to the patient's immune status (78,79). Lesions of the corpus callosum, basal ganglia, and thalami may be seen, because of involvement of the perforating arteries. On diffusion-weighted images, low ADC values are observed within the fungal abscesses. Luthra et al (80) found that diffusion-weighted images and

Teaching Point

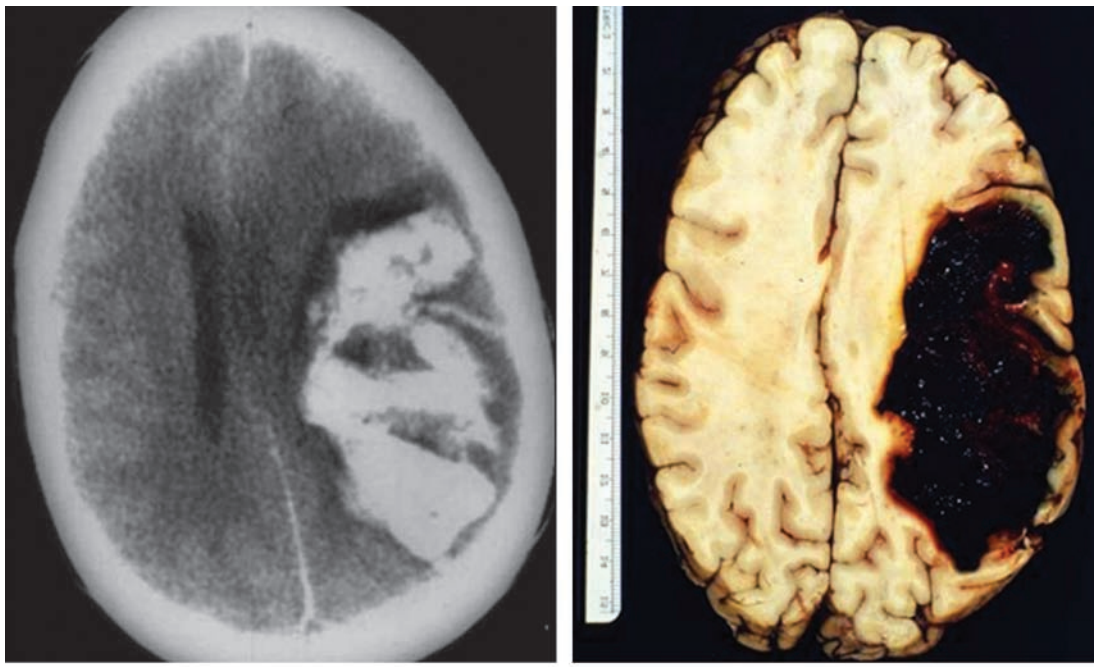

a. b.

Figure 17. Aspergillosis in a 36-year-old woman with HIV infection who experienced a rapid decline in consciousness. **(a)** Axial unenhanced CT image reveals a large parenchymal hemorrhage involving the left hemisphere that caused mass effect and midline shift. **(b)** Photograph of the gross specimen demonstrates the large area of hemorrhage.

ADC values demonstrated reduced diffusion in the projections and wall of the fungal abscess, whereas the core of the abscess did not exhibit reduced diffusion, a pattern unlike that demonstrated by pyogenic and tuberculous abscesses.

Differential Diagnosis.—The CT and MR imaging findings of invasive aspergillosis are indistinguishable from those of other fungal infections, such as mucormycosis, that occur in immunocompromised patients. Both of these fungi may mimic aggressive tumors at CT and MR imaging. They may also appear similar to pyogenic and tuberculous abscesses.

Treatment and Prognosis.—The fatality rate for CNS aspergillosis is reported to be as high as 88% (81). Prevention of the infection is the optimal therapy at this time, because the current treatment of cerebral aspergillosis is limited (82).

Tuberculosis

Tuberculosis has seen a resurgence in the past two decades because of the increasing numbers of AIDS patients. CNS tuberculosis is an AIDS-defining illness, and it may be the initial clinical manifestation of AIDS. CNS tuberculosis can result from reactivation of a previous infection or from a primary, newly acquired infection.

Epidemiology and Clinical Features

In 2004, 250,000 of the 1.7 million patients worldwide who died of tuberculosis were infected with HIV (83). CNS tuberculosis has a high mortality rate of at least 70%. A total of 5%–9% of AIDS patients develop tuberculosis, and of these, 2%–18% will have CNS infection (84–86). Results from chest radiography will be positive in 65% of these patients. The predominant mechanism of disease spread is hematogenous.

Pathologic Features

The most common intracranial manifestation of tuberculosis is meningitis, which is usually more prominent in the basilar cisterns, especially around the circle of Willis. However, tuberculomas, tuberculous abscess, and cerebral ischemia and infarction are not uncommon findings. HIV infection may alter the pathologic features of tuberculous meningitis. Fewer basal exudates and greater numbers of acid-fast bacilli occur in the brain parenchyma and meninges in patients with HIV infection (Fig 18a) (87).

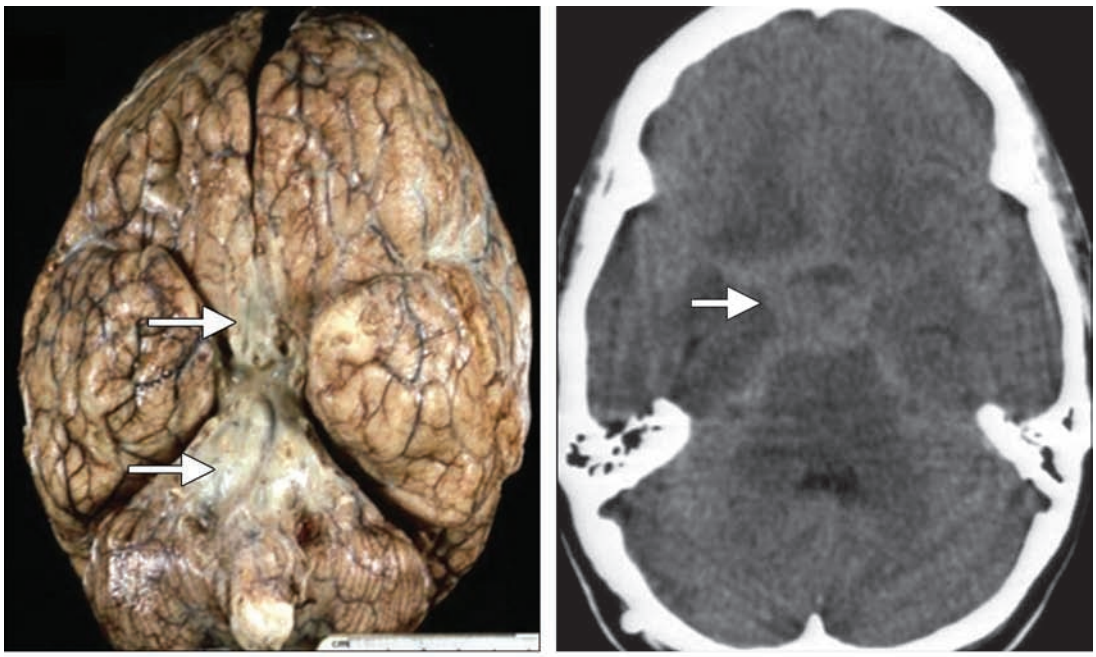

a. b.

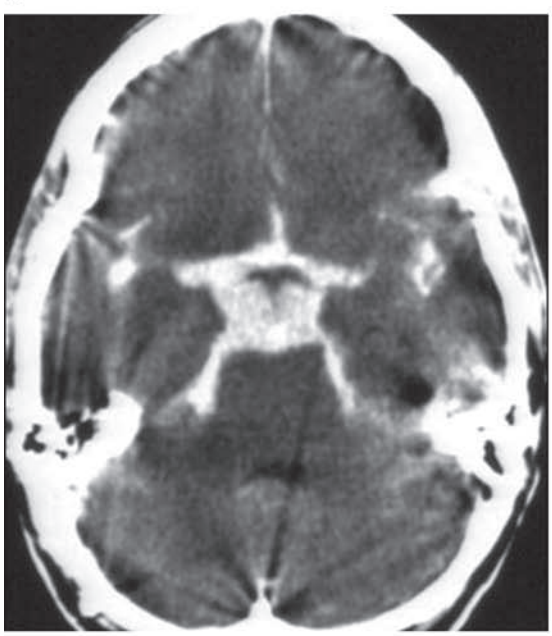

c.

Figure 18. Tuberculosis basilar meningitis in a 30-year-old woman with HIV infection. **(a)** Photograph of a gross specimen reveals thick purulent exudate, most predominantly in the basilar cisterns and anterior to the pons (arrows), a finding consistent with meningitis. **(b)** Unenhanced axial CT image shows high-attenuation material in the basilar cisterns (arrow). **(c)** Axial postcontrast CT image reveals avid enhancement in the basilar cisterns.

Tuberculomas are composed of a central zone of solid caseation necrosis that is surrounded by collagenous tissue, epitheloid histiocytes, Langhans-type multinucleated giant cells, and mononuclear inflammatory cells. Smears demonstrate few bacilli.

Imaging Features

In one study, hydrocephalus was seen in 51% and meningeal enhancement in 45% of patients with CNS tuberculosis (Fig 18b, 18c) (85). The hydrocephalus results primarily from obstruction of the basal cistern by inflammatory exudate. In addition, cerebral abscesses and tuberculomas may be seen (85). Tuberculomas occurred in 24% of patients in a study by Whiteman et al (84). Tuberculomas are granulomas that result either from hematogenous spread or extension from cerebrospinal fluid infection via cortical veins or small penetrating arteries (84). The majority of tuberculomas are supratentorial and may be solitary or multiple; however, they can also be found in subdural, epidural, and subarachnoid spaces (Fig 19) (84). Tuberculomas are hypointense on T2-weighted MR images in the early stages; as they mature, they develop a hypointense center surrounded by an isointense capsule, which corresponds to solid caseation necrosis. They may further progress to abscess formation with a hyperintense center. However, some tuberculomas have a hyperintense center without abscess formation, an appearance that makes them difficult to distinguish from lesions of toxoplasmosis or

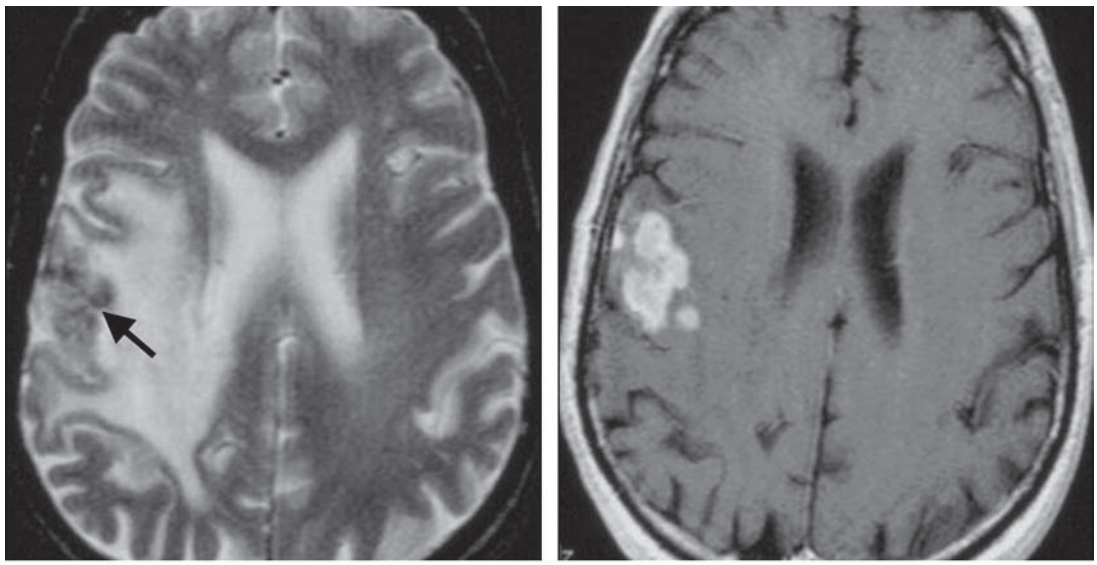

a. b.

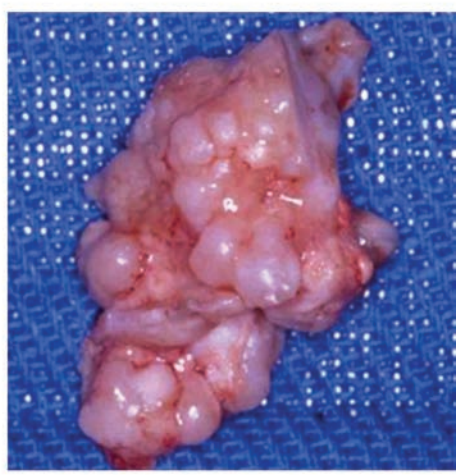

c.

Figure 19. Tuberculoma in a 32-year-old man with HIV infection who presented with headache. **(a)** Axial T2-weighted image demonstrates small, peripherally located, low-signal-intensity lesions (arrow) with surrounding vasogenic edema. **(b)** Axial postcontrast T1-weighted image shows multiple small, separate and confluent, avidly enhancing lesions. **(c)** Photograph of the resected gross specimen reveals a nodular mass.

lymphoma. Associated findings of hydrocephalus, basal ganglia infarction, and cisternal enhancement should help one distinguish among these entities, since these findings are typically not encountered in lymphoma and toxoplasmosis. On postcontrast images, noncaseating tuberculomas demonstrate nodular homogeneous enhancement. Caseating tuberculomas have ring enhancement.

Tuberculous abscesses are more common in HIV-infected patients. Among patients with CNS tuberculosis, 4%–8% of those without HIV infection developed abscesses, compared with up to 20% in one group of HIV patients (84). Abscesses tend to be larger—frequently greater than 3 cm—than tuberculomas, which are typically less than 1 cm (84). Abscesses are also more frequently solitary than tuberculomas. Similar to other abscesses, tuberculous abscesses demonstrate ring enhancement after administration of contrast material. At MR spectroscopy, they demonstrate prominent lipid and lactate peaks, but no amino acid peak, unlike bacterial abscesses (88).

Cerebral infarction complicates CNS tuberculosis and was seen in 36% of the patients in the study by Whiteman et al (84). Vasospasm and thrombosis of arteries as they course through the thick basilar exudate result in infarctions of the small perforating arteries that supply the basal ganglia (89). Diffusion-weighted imaging may be helpful in detecting complications from tuberculosis, such as infarction or cerebritis.

Treatment and Prognosis

Tuberculous meningitis is the most lethal infection associated with CNS tuberculosis, with a mortality rate of approximately 30% (90,91). Infected patients are typically treated with steroids in addition to antituberculin drugs.

Neurosyphilis

Neurosyphilis is a sexually transmitted disease that results from infection with the spirochete *Treponema pallidum*. A resurgence of this entity has been seen among the HIV-infected population.

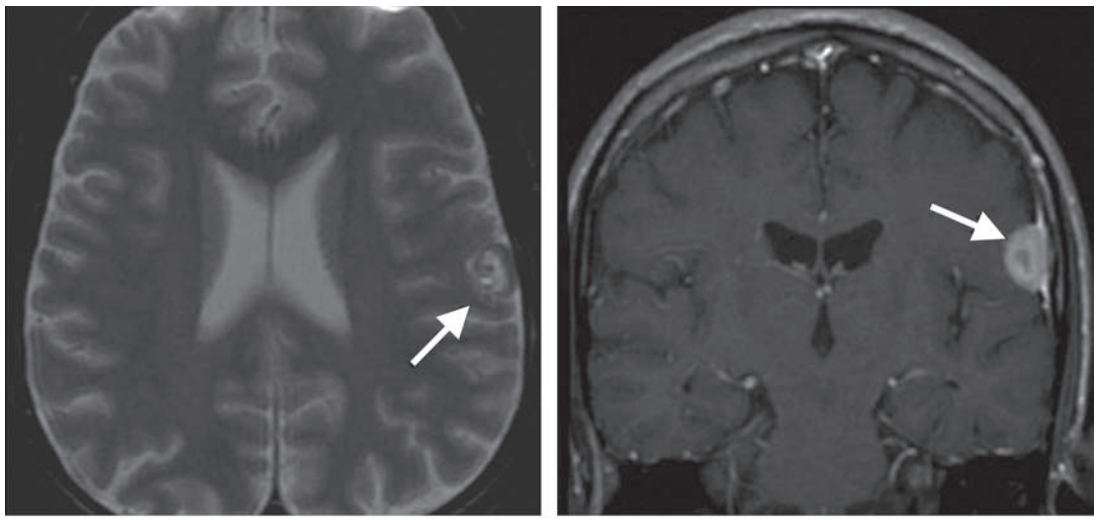

a. b.

Figure 20. Syphilitic gumma in a 32-year-old man with HIV infection and a positive VDRL test. **(a)** Axial T2-weighted image shows an extraaxial, predominantly hyperintense lesion with a central focus of low signal intensity (arrow). **(b)** On a coronal postcontrast T1-weighted image, the lesion heterogeneously enhances and demonstrates a mild degree of dural enhancement. (Case courtesy of Max Wintermark, MD, University of California, San Francisco.)

Epidemiology and Clinical Features

Neurosyphilis affects approximately 1.5% of the AIDS population. In this population, it has a shorter latent period for progression to clinically evident neurologic disease (92). CNS involvement occurs in 5%–10% of untreated patients and may occur at any stage of the syphilitic infection (93,94). Because many patients with neurosyphilis are asymptomatic or have nonspecific symptoms, such as headaches, seizures, personality change, and confusion, diagnosis can be difficult (95,96). Symptomatic cases can be divided into four types based on the predominant clinical features: meningeal, vascular, general paresis, and tabes dorsalis. The most common forms of neurosyphilis are the meningeal and vascular, whereas general paresis and tabes dorsalis are rare in the era of antibiotics. Symptoms occurring with the meningeal form resemble those of any acute meningitis: headache, cranial neuritis, and hydrocephalus. This form usually occurs in the first 2 years of infection (97). Vascular syphilis typically occurs 5–7 years after the primary infection and is characterized by headache, transient hemiparesis, and abnormal cerebrospinal fluid findings (93). Laboratory findings in neurosyphilis include positive results from a serum fluorescent antibody test, pleocytosis, elevated protein levels, or a positive VDRL test. If the cerebrospinal fluid VDRL is positive, it is highly specific for neurosyphilis, but this test is negative in approximately one-half of neurosyphilis patients.

Pathologic Features

Patients may develop leptomeningitis and multifocal arteritis, conditions that potentially lead to cerebral infarction. Both small vessel endarteritis and large and medium-sized vessel arteritis occur. Other findings include nonspecific white matter lesions and cerebral gummas. Gummas represent well-circumscribed masses of necrosis in which reticulin is preserved. Cerebral gummas are characterized by infiltration of the meninges and brain by lymphocytes and abundant plasma cells. Eventually, these cells are replaced by fibrosis and necrosis. Spirochetes are not typically found in these lesions (98).

Imaging Features

Neurosyphilis has a wide variety of imaging findings. Mild to moderate atrophy, white matter lesions, cortical and subcortical infarctions, gummas, leptomeningeal enhancement, and arteritis have all been reported (94,95). Gummas are uncommon. They are usually located peripherally in the cerebral hemisphere cortex. On CT images, they appear as peripherally located lesions that are isoattenuating relative to the cortex. On MR images, they are isointense relative to gray matter with T1-weighted sequences and hyperintense with T2-weighted sequences. These lesions will enhance with contrast material (Fig 20). Overlying leptomeningeal enhancement may also be seen.

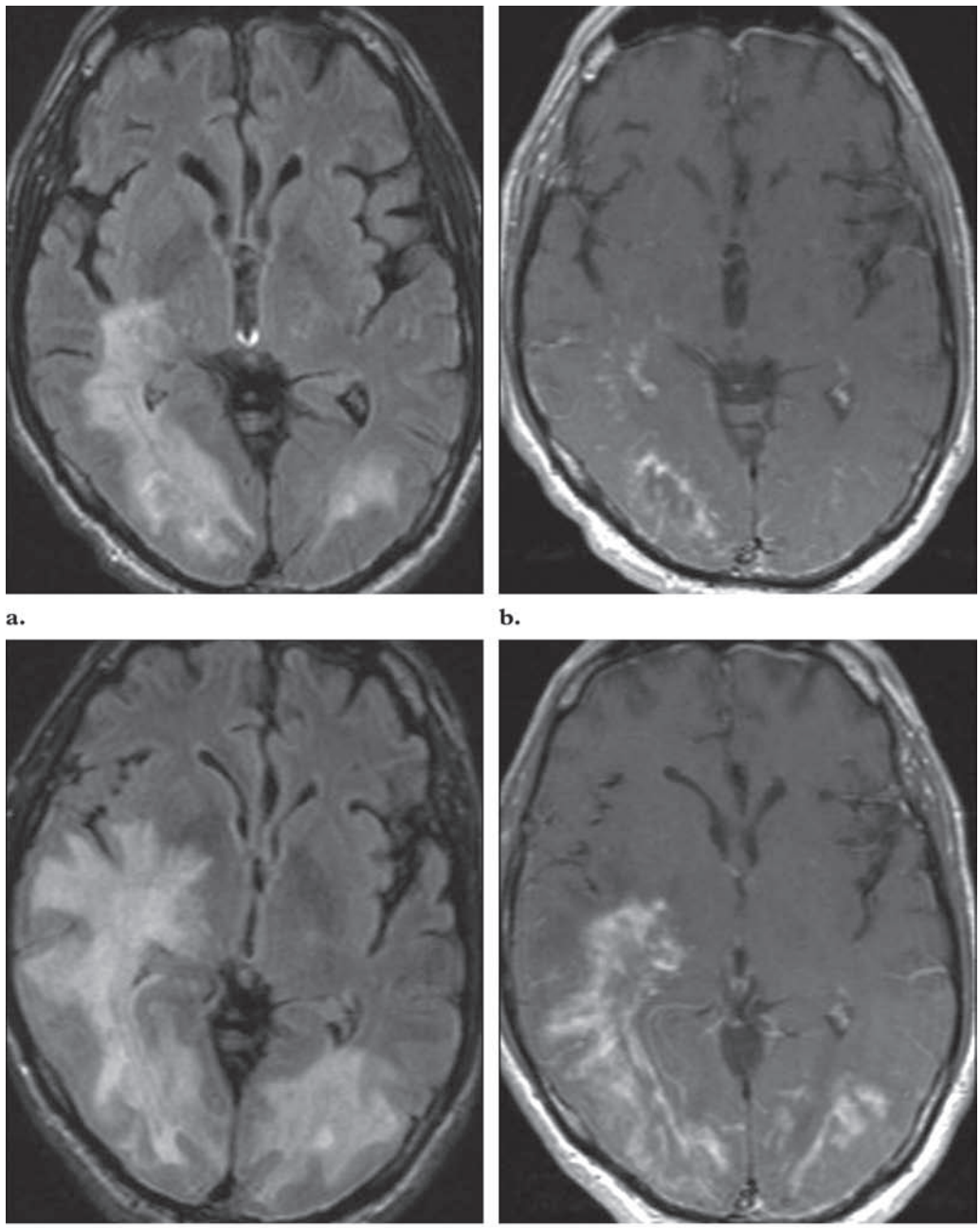

Figure 21. IRIS in a patient with biopsy-proved PML. **(a)** Axial T2-weighted FLAIR image demonstrates T2 hyperintensity in the bilateral (right greater than left) periatrial white matter. **(b)** Axial postcontrast T1-weighted image reveals diffuse patchy enhancement in the region of the T2 hyperintensity. **(c)** Axial T2-weighted FLAIR image obtained 2 weeks later demonstrates progression of the T2 hyperintensity, with an increase in mass effect. **(d)** Axial postcontrast T1-weighted image reveals progression of the patchy enhancement in the 2-week interval. (Case courtesy of Max Wintermark, MD, University of California, San Francisco.)

On MR images, regions of nonspecific T2 hyperintensity may be seen in the white matter. There have been reports of neurosyphilis that demonstrates mesiotemporal T2-weighted hyperintensity, a finding that mimics herpes encephalitis (96,99,100). Evidence of infarctions of various ages may be seen, and meningovascular syphilis should always be in the differential diagnosis for an HIV-infected patient who presents with cerebral infarction. The infarcts are typically located in the perforating artery territory of the basal ganglia

and brainstem. The middle cerebral artery territory is another common location. The cranial nerves, especially the optic and vestibulocochlear nerves, have also been reported to be involved.

Treatment and Prognosis

The course of neurosyphilis in HIV-infected patients tends to be more aggressive than it is in the general population. Early diagnosis is critical for disease management because the infection is easily treatable with antibiotics.

Bacterial Infections

Pyogenic intracranial infections are relatively uncommon in the AIDS population. AIDS patients are subject to the same types of bacterial infections seen in immunocompetent patients, and *Staphylococcus* and *Streptococcus* are the most common causative organisms. The imaging findings seen in AIDS patients are identical to those seen in immunocompetent patients.

Immune Reconstitution Inflammatory Syndrome

HAART succeeds in suppressing HIV replication and improving cellular immunity, which protects HIV-infected patients against opportunistic infections (101). However, in a few of these patients, partial restoration of specific immunity may worsen a preexisting disease; the resulting condition is referred to as immune reconstitution inflammatory syndrome (IRIS) (102). IRIS is not caused by a relapse or recurrence of the preexisting disease, and its exact etiology is unknown. IRIS is thought to be related to reconstitution of immunity, which leads to abnormal immune response to either specific infectious or noninfectious antigens (103). Patients with IRIS demonstrate paradoxic deterioration in their clinical status when their CD4 counts rise and viral replication appears to be under control (102), and death from IRIS has been reported (17). IRIS occurs in the initial months after the onset of HAART. The neuroimaging findings vary, depending on the underlying pathologic conditions, and may be atypical, such as prominent, progressive enhancement and mass effect seen in PML (Fig 21).

Conclusions

The neuroimaging findings of infectious CNS diseases in patients with HIV infection are varied, including mass lesions, atrophy, demyelination, vascular complications, and meningoencephalitis. HAART has led to improvement of many of the imaging findings, but it can occasionally result in IRIS, which has atypical imaging findings. Knowledge of the imaging findings of infectious CNS diseases in HIV-infected patients, as well as the impact of HAART, is important in patient treatment.

References

1. World Health Organization, Joint United Nations Programme on HIV/AIDS. AIDS epidemic update: December 2006. Geneva, Switzerland: World Health Organization, 2006.
2. Gray F, Scaravilli F, Everall I, et al. Neuropathology of early HIV-1 infection. Brain Pathol 1996;6 (1):1–15.
3. An SF, Giometto B, Scaravilli F. HIV-1 DNA in brains in AIDS and pre-AIDS: correlation with the stage of disease. Ann Neurol 1996;40(4):611–617.
4. Levy RM, Bredesen DE, Rosenblum ML. Neurological manifestations of the acquired immunodeficiency syndrome (AIDS): experience at UCSF and review of the literature. J Neurosurg 1985;62(4): 475–495.
5. de la Monte SM, Ho DD, Schooley RT, Hirsch MS, Richardson EP Jr. Subacute encephalomyelitis of AIDS and its relation to HTLV-III infection. Neurology 1987;37(4):562–569.
6. Chiodi F, Keys B, Albert J, et al. Human immunodeficiency virus type 1 is present in the cerebrospinal fluid of a majority of infected individuals. J Clin Microbiol 1992;30(7):1768–1771.
7. Garcia F, Plana M, Vidal C, et al. Dynamics of viral load rebound and immunological changes after stopping effective antiretroviral therapy. AIDS 1999; 13(11):F79–F86.
8. Saito Y, Sharer LR, Epstein LG, et al. Overexpression of nef as a marker for restricted HIV-1 infection of astrocytes in postmortem pediatric central nervous tissues. Neurology 1994;44(3 pt 1):474–481.
9. Tornatore C, Chandra R, Berger JR, Major EO. HIV-1 infection of subcortical astrocytes in the pediatric central nervous system. Neurology 1994;44 (3 pt 1):481–487.
10. Kaplan JE, Masur H, Holmes KK. Guidelines for preventing opportunistic infections among HIV-infected persons–2002: recommendations of the U.S. Public Health Service and the Infectious Diseases Society of America. MMWR Recomm Rep 2002;51 (RR-8):1–52.
11. Brodt HR, Kamps BS, Gute P, Knupp B, Staszewski S, Helm EB. Changing incidence of AIDS-defining illnesses in the era of antiretroviral combination therapy. AIDS 1997;11(14):1731–1738.
12. Maschke M, Kastrup O, Esser S, Ross B, Hengge U, Hufnagel A. Incidence and prevalence of neurological disorders associated with HIV since the introduction of highly active antiretroviral therapy (HAART). J Neurol Neurosurg Psychiatry 2000;69 (3):376–380.
13. McArthur JC, Sacktor N, Selnes O. Human immunodeficiency virus-associated dementia. Semin Neurol 1999;19(2):129–150.
14. Bouwman FH, Skolasky RL, Hes D, et al. Variable progression of HIV-associated dementia. Neurology 1998;50(6):1814–1820.

15. Achim CL, Wang R, Miners DK, Wiley CA. Brain viral burden in HIV infection. J Neuropathol Exp Neurol 1994;53(3):284–294.
16. Bhaskaran K, Mussini C, Antinori A, et al. Changes in the incidence and predictors of human immunodeficiency virus-associated dementia in the era of highly active antiretroviral therapy. Ann Neurol 2008;63(2):213–221.
17. Langford TD, Letendre SL, Larrea GJ, Masliah E. Changing patterns in the neuropathogenesis of HIV during the HAART era. Brain Pathol 2003; 13(2):195–210.
18. Persidsky Y, Stins M, Way D, et al. A model for monocyte migration through the blood-brain barrier during HIV-1 encephalitis. J Immunol 1997; 158(7):3499–3510.
19. Masliah E, Achim CL, Ge N, DeTeresa R, Terry RD, Wiley CA. Spectrum of human immunodeficiency virus-associated neocortical damage. Ann Neurol 1992;32(3):321–329.
20. Lackner AA, Smith MO, Munn RJ, et al. Localization of simian immunodeficiency virus in the central nervous system of rhesus monkeys. Am J Pathol 1991;139(3):609–621.
21. Budka H. Neuropathology of human immunodeficiency virus infection. Brain Pathol 1991;1(3): 163–175.
22. Scaravilli F, Bazille C, Gray F. Neuropathologic contributions to understanding AIDS and the central nervous system. Brain Pathol 2007;17(2):197–208.
23. Ciardi A, Sinclair E, Scaravilli F, Harcourt-Webster NJ, Lucas S. The involvement of the cerebral cortex in human immunodeficiency virus encephalopathy: a morphological and immunohistochemical study. Acta Neuropathol 1990;81(1):51–59.
24. Patel SH, Inglese M, Glosser G, Kolson DL, Grossman RI, Gonen O. Whole-brain N-acetylaspartate level and cognitive performance in HIV infection. AJNR Am J Neuroradiol 2003;24(8):1587–1591.
25. Laubenberger J, Haussinger D, Bayer S, et al. HIV-related metabolic abnormalities in the brain: depiction with proton MR spectroscopy with short echo times. Radiology 1996;199(3):805–810.
26. Thurnher MM, Post MJ, Rieger A, Kleibl-Popov C, Loewe C, Schindler E. Initial and follow-up MR imaging findings in AIDS-related progressive multifocal leukoencephalopathy treated with highly active antiretroviral therapy. AJNR Am J Neuroradiol 2001;22(5):977–984.
27. Pomara N, Crandall DT, Choi SJ, Johnson G, Lim KO. White matter abnormalities in HIV-1 infection: a diffusion tensor imaging study. Psychiatry Res 2001;106(1):15–24.
28. Filippi CG, Ulug AM, Ryan E, Ferrando SJ, van Gorp W. Diffusion tensor imaging of patients with HIV and normal-appearing white matter on MR images of the brain. AJNR Am J Neuroradiol 2001; 22(2):277–283.
29. Dore GJ, McDonald A, Li Y, Kaldor JM, Brew BJ. Marked improvement in survival following AIDS dementia complex in the era of highly active antiretroviral therapy. AIDS 2003;17(10):1539–1545.
30. Hogan TF, Padgett BL, Walker DL, Borden EC, McBain JA. Rapid detection and identification of JC virus and BK virus in human urine by using immunofluorescence microscopy. J Clin Microbiol 1980;11(2):178–183.
31. Petito CK, Cho ES, Lemann W, Navia BA, Price RW. Neuropathology of acquired immunodeficiency syndrome (AIDS): an autopsy review. J Neuropathol Exp Neurol 1986;45(6):635–646.
32. Berger JR, Levy RM, Flomenhoft D, Dobbs M. Predictive factors for prolonged survival in acquired immunodeficiency syndrome-associated progressive multifocal leukoencephalopathy. Ann Neurol 1998; 44(3):341–349.
33. McGuire D, Barhite S, Hollander H, Miles M. JC virus DNA in cerebrospinal fluid of human immunodeficiency virus-infected patients: predictive value for progressive multifocal leukoencephalopathy. Ann Neurol 1995;37(3):395–399.
34. Fong IW, Britton CB, Luinstra KE, Toma E, Mahony JB. Diagnostic value of detecting JC virus DNA in cerebrospinal fluid of patients with progressive multifocal leukoencephalopathy. J Clin Microbiol 1995;33(2):484–486.
35. Marzocchetti A, Di Giambenedetto S, Cingolani A, Ammassari A, Cauda R, De Luca A. Reduced rate of diagnostic positive detection of JC virus DNA in cerebrospinal fluid in cases of suspected progressive multifocal leukoencephalopathy in the era of potent antiretroviral therapy. J Clin Microbiol 2005;43(8):4175–4177.
36. Whiteman ML, Post MJ, Berger JR, Tate LG, Bell MD, Limonte LP. Progressive multifocal leukoencephalopathy in 47 HIV-seropositive patients: neuroimaging with clinical and pathologic correlation. Radiology 1993;187(1):233–240.
37. Wheeler AL, Truwit CL, Kleinschmidt-DeMasters BK, Byrne WR, Hannon RN. Progressive multifocal leukoencephalopathy: contrast enhancement on CT scans and MR images. AJR Am J Roentgenol 1993;161(5):1049–1051.
38. Port JD, Miseljic S, Lee RR, et al. Progressive multifocal leukoencephalopathy demonstrating contrast enhancement on MRI and uptake of thallium-201: a case report. Neuroradiology 1999;41(12):895–898.
39. Kotecha N, George MJ, Smith TW, Corvi F, Litofsky NS. Enhancing progressive multifocal leukoencephalopathy: an indicator of improved immune status? Am J Med 1998;105(6):541–543.
40. Arbusow V, Strupp M, Pfister HW, Seelos KC, Bruckmann H, Brandt T. Contrast enhancement in progressive multifocal leukoencephalopathy: a predictive factor for long-term survival? J Neurol 2000;247(4):306–308.
41. Collazos J, Mayo J, Martinez E, Blanco MS. Contrast-enhancing progressive multifocal leukoencephalopathy as an immune reconstitution event in AIDS patients. AIDS 1999;13(11):1426–1428.
42. Ohta K, Obara K, Sakauchi M, Obara K, Takane H, Yogo Y. Lesion extension detected by diffusion-weighted magnetic resonance imaging in progressive multifocal leukoencephalopathy. J Neurol 2001;248(9):809–811.

43. Usiskin SI, Bainbridge A, Miller RF, Jager HR. Progressive multifocal leukoencephalopathy: serial high-b-value diffusion-weighted MR imaging and apparent diffusion coefficient measurements to assess response to highly active antiretroviral therapy. AJNR Am J Neuroradiol 2007;28(2):285–286.
44. Levy RM, Mills CM, Posin JP, Moore SG, Rosenblum ML, Bredesen DE. The efficacy and clinical impact of brain imaging in neurologically symptomatic AIDS patients: a prospective CT/MRI study. J Acquir Immune Defic Syndr 1990;3(5):461–471.
45. Cornford ME, Holden JK, Boyd MC, Berry K, Vinters HV. Neuropathology of the acquired immune deficiency syndrome (AIDS): report of 39 autopsies from Vancouver, Br Columbia. Can J Neurol Sci 1992;19(4):442–452.
46. Wright D, Schneider A, Berger JR. Central nervous system opportunistic infections. Neuroimaging Clin N Am 1997;7(3):513–525.
47. Ammassari A, Cingolani A, Pezzotti P, et al. AIDS-related focal brain lesions in the era of highly active antiretroviral therapy. Neurology 2000;55(8): 1194–1200.
48. Luft BJ, Remington JS. Toxoplasmic encephalitis in AIDS. Clin Infect Dis 1992;15(2):211–222.
49. Zufferey J, Sugar A, Rudaz P, Bille J, Glauser MP, Chave JP. Prevalence of latent toxoplasmosis and serological diagnosis of active infection in HIV-positive patients. Eur J Clin Microbiol Infect Dis 1993;12(8):591–595.
50. Colombo FA, Vidal JE, Penalva de Oliveira AC, et al. Diagnosis of cerebral toxoplasmosis in AIDS patients in Brazil: importance of molecular and immunological methods using peripheral blood samples. J Clin Microbiol 2005;43(10):5044–5047.
51. Navia BA, Petito CK, Gold JW, Cho ES, Jordan BD, Price RW. Cerebral toxoplasmosis complicating the acquired immune deficiency syndrome: clinical and neuropathological findings in 27 patients. Ann Neurol 1986;19(3):224–238.
52. Trenkwalder P, Trenkwalder C, Feiden W, Vogl TJ, Einhaupl KM, Lydtin H. Toxoplasmosis with early intracerebral hemorrhage in a patient with the acquired immunodeficiency syndrome. Neurology 1992;42(2):436–438.
53. Fischbein NJ, Dillon WP, Barkovich AJ. Teaching atlas of brain imaging. New York, NY: Thieme, 2000.
54. Lee HJ, Williams R, Kalnin A, Wolansky L. Toxoplasmosis of the corpus callosum: another butterfly. AJR Am J Roentgenol 1996;166(6):1280–1281.
55. Dina TS. Primary central nervous system lymphoma versus toxoplasmosis in AIDS. Radiology 1991;179 (3):823–828.
56. Skiest DJ, Erdman W, Chang WE, Oz OK, Ware A, Fleckenstein J. SPECT thallium-201 combined with Toxoplasma serology for the presumptive diagnosis of focal central nervous system mass lesions in patients with AIDS. J Infect 2000;40(3):274–281.
57. Lorberboym M, Wallach F, Estok L, et al. Thallium-201 retention in focal intracranial lesions for differential diagnosis of primary lymphoma and nonmalignant lesions in AIDS patients. J Nucl Med 1998; 39(8):1366–1369.
58. Licho R, Litofsky NS, Senitko M, George M. Inaccuracy of Tl-201 brain SPECT in distinguishing cerebral infections from lymphoma in patients with AIDS. Clin Nucl Med 2002;27(2):81–86.
59. Pomper MG, Constantinides CD, Barker PB, et al. Quantitative MR spectroscopic imaging of brain lesions in patients with AIDS: correlation with [11C-methyl]thymidine PET and thallium-201 SPECT. Acad Radiol 2002;9(4):398–409.
60. Chang L, Miller BL, McBride D, et al. Brain lesions in patients with AIDS: H-1 MR spectroscopy. Radiology 1995;197(2):525–531.
61. Ionita C, Wasay M, Balos L, Bakshi R. MR imaging in toxoplasmosis encephalitis after bone marrow transplantation: paucity of enhancement despite fulminant disease. AJNR Am J Neuroradiol 2004; 25(2):270–273.
62. Schroeder PC, Post MJ, Oschatz E, Stadler A, Bruce-Gregorios J, Thurnher MM. Analysis of the utility of diffusion-weighted MRI and apparent diffusion coefficient values in distinguishing central nervous system toxoplasmosis from lymphoma. Neuroradiology 2006;48(10):715–720.
63. Arribas JR, Storch GA, Clifford DB, Tselis AC. Cytomegalovirus encephalitis. Ann Intern Med 1996;125(7):577–587.
64. McNeil MM, Nash SL, Hajjeh RA, et al. Trends in mortality due to invasive mycotic diseases in the United States, 1980–1997. Clin Infect Dis 2001; 33(5):641–647.
65. Kume H, Yamazaki T, Abe M, Tanuma H, Okudaira M, Okayasu I. Increase in aspergillosis and severe mycotic infection in patients with leukemia and MDS: comparison of the data from the Annual of the Pathological Autopsy Cases in Japan in 1989, 1993 and 1997. Pathol Int 2003;53(11):744–750.
66. Pagano L, Gleissner B, Fianchi L. Breakthrough zygomycosis and voriconazole. J Infect Dis 2005; 192(8):1496–1497; author reply 1497.
67. Sabetta JR, Andriole VT. Cryptococcal infection of the central nervous system. Med Clin North Am 1985;69(2):333–344.
68. Zuger A, Louie E, Holzman RS, Simberkoff MS, Rahal JJ. Cryptococcal disease in patients with the acquired immunodeficiency syndrome: diagnostic features and outcome of treatment. Ann Intern Med 1986;104(2):234–240.
69. Eng RH, Bishburg E, Smith SM, Kapila R. Cryptococcal infections in patients with acquired immune deficiency syndrome. Am J Med 1986;81(1):19–23.
70. Mamidi A, DeSimone JA, Pomerantz RJ. Central nervous system infections in individuals with HIV-1 infection. J Neurovirol 2002;8(3):158–167.
71. Mathews VP, Alo PL, Glass JD, Kumar AJ, McArthur JC. AIDS-related CNS cryptococcosis: radiologic-pathologic correlation. AJNR Am J Neuroradiol 1992;13(5):1477–1486.
72. Takasu A, Taneda M, Otuki H, Okamoto Y, Oku K. Gd-DTPA-enhanced MR imaging of cryptococcal meningoencephalitis. Neuroradiology 1991;33(5): 443–446.

73. Ho TL, Lee HJ, Lee KW, Chen WL. Diffusion-weighted and conventional magnetic resonance imaging in cerebral cryptococcoma. Acta Radiol 2005; 46(4):411–414.
74. Vender JR, Miller DM, Roth T, Nair S, Reboli AC. Intraventricular cryptococcal cysts. AJNR Am J Neuroradiol 1996;17(1):110–113.
75. Tien RD, Chu PK, Hesselink JR, Duberg A, Wiley C. Intracranial cryptococcosis in immunocompromised patients: CT and MR findings in 29 cases. AJNR Am J Neuroradiol 1991;12(2):283–289.
76. Mathews M, Pare L, Hasso A. Intraventricular cryptococcal cysts masquerading as racemose neurocysticercosis. Surg Neurol 2007;67(6):647–649.
77. Robinson PA, Bauer M, Leal MA, et al. Early mycological treatment failure in AIDS-associated cryptococcal meningitis. Clin Infect Dis 1999;28 (1): 82–92.
78. Ashdown BC, Tien RD, Felsberg GJ. Aspergillosis of the brain and paranasal sinuses in immunocompromised patients: CT and MR imaging findings. AJR Am J Roentgenol 1994;162(1):155–159.
79. DeLone DR, Goldstein RA, Petermann G, et al. Disseminated aspergillosis involving the brain: distribution and imaging characteristics. AJNR Am J Neuroradiol 1999;20(9):1597–1604.
80. Luthra G, Parihar A, Nath K, et al. Comparative evaluation of fungal, tubercular, and pyogenic brain abscesses with conventional and diffusion MR imaging and proton MR spectroscopy. AJNR Am J Neuroradiol 2007;28(7):1332–1338.
81. Lin SJ, Schranz J, Teutsch SM. Aspergillosis case-fatality rate: systematic review of the literature. Clin Infect Dis 2001;32(3):358–366.
82. Steinbach WJ, Stevens DA, Denning DW. Combination and sequential antifungal therapy for invasive aspergillosis: review of published in vitro and in vivo interactions and 6281 clinical cases from 1966 to 2001. Clin Infect Dis 2003;37(suppl 3): S188–S224.
83. World Health Organization. Global tuberculosis control: surveillance, planning, financing. Geneva, Switzerland: World Health Organization, 2006.
84. Whiteman M, Espinoza L, Post MJ, Bell MD, Falcone S. Central nervous system tuberculosis in HIV-infected patients: clinical and radiographic findings. AJNR Am J Neuroradiol 1995;16(6): 1319–1327.
85. Villoria MF, de la Torre J, Fortea F, Munoz L, Hernandez T, Alarcon JJ. Intracranial tuberculosis in AIDS: CT and MRI findings. Neuroradiology 1992;34(1):11–14.
86. Bishburg E, Sunderam G, Reichman LB, Kapila R. Central nervous system tuberculosis with the acquired immunodeficiency syndrome and its related complex. Ann Intern Med 1986;105(2): 210–213.
87. Katrak SM, Shembalkar PK, Bijwe SR, Bhandarkar LD. The clinical, radiological and pathological profile of tuberculous meningitis in patients with and without human immunodeficiency virus infection. J Neurol Sci 2000;181(1–2):118–126.
88. Gupta RK, Vatsal DK, Husain N, et al. Differentiation of tuberculous from pyogenic brain abscesses with in vivo proton MR spectroscopy and magnetization transfer MR imaging. AJNR Am J Neuroradiol 2001;22(8):1503–1509.
89. Sheller JR, Des Prez RM. CNS tuberculosis. Neurol Clin 1986;4(1):143–158.
90. Thwaites GE, Tran TH. Tuberculous meningitis: many questions, too few answers. Lancet Neurol 2005;4(3):160–170.
91. Garg RK. Tuberculosis of the central nervous system. Postgrad Med J 1999;75(881):133–140.
92. Johns DR, Tierney M, Felsenstein D. Alteration in the natural history of neurosyphilis by concurrent infection with the human immunodeficiency virus. N Engl J Med 1987;316(25):1569–1572.
93. Holland BA, Perrett LV, Mills CM. Meningovascular syphilis: CT and MR findings. Radiology 1986; 158(2):439–442.
94. Brightbill TC, Ihmeidan IH, Post MJ, Berger JR, Katz DA. Neurosyphilis in HIV-positive and HIV-negative patients: neuroimaging findings. AJNR Am J Neuroradiol 1995;16(4):703–711.
95. Harris DE, Enterline DS, Tien RD. Neurosyphilis in patients with AIDS. Neuroimaging Clin N Am 1997;7(2):215–221.
96. Bash S, Hathout GM, Cohen S. Mesiotemporal T2-weighted hyperintensity: neurosyphilis mimicking herpes encephalitis. AJNR Am J Neuroradiol 2001;22(2):314–316.
97. Simon RP. Neurosyphilis. Arch Neurol 1985;42 (6): 606–613.
98. Berger JR, Waskin H, Pall L, Hensley G, Ihmedian I, Post MJ. Syphilitic cerebral gumma with HIV infection. Neurology 1992;42(7):1282–1287.
99. Denays R, Collier A, Rubinstein M, Atsama P. A 51-year-old woman with disorientation and amnesia. Lancet 1999;354(9192):1786.
100. Angus F, Maysuria H, Bryan CS. Neurosyphilis mimicking herpes simplex encephalitis. J S C Med Assoc 1998;94(7):315–317.
101. Autran B, Carcelain G, Li TS, et al. Positive effects of combined antiretroviral therapy on CD4+ T cell homeostasis and function in advanced HIV disease. Science 1997;277(5322):112–116.
102. Shelburne SA 3rd, Hamill RJ, Rodriguez-Barradas MC, et al. Immune reconstitution inflammatory syndrome: emergence of a unique syndrome during highly active antiretroviral therapy. Medicine (Baltimore) 2002;81(3):213–227.
103. Michailidis C, Pozniak AL, Mandalia S, Basnayake S, Nelson MR, Gazzard BG. Clinical characteristics of IRIS syndrome in patients with HIV and tuberculosis. Antivir Ther 2005;10(3):417–422.

This article meets the criteria for 1.0 credit hour in category 1 of the AMA Physician's Recognition Award. To obtain credit, see accompanying test at http://www.rsna.org/education/rg_cme.html.

Central Nervous System Infections Associated with Human Immunodeficiency Virus Infection: Radiologic-Pathologic Correlation

Alice B. Smith, MD, et al

RadioGraphics 2008; 28:2033–2058 • **Published online** 10.1148/rg.287085135 • **Content Code:** NR

Page 2035
HIV encephalopathy does not result in mass effect or enhancement. If either of these findings is present, another diagnosis must be considered.

Page 2039
In patients with PML, CT reveals asymmetric focal zones of low attenuation that involve the periventricular and subcortical white matter (Fig 4a). This appearance is a differential diagnostic feature compared with the typically more symmetric areas of low attention seen in patients with HIV encephalopathy.

Page 2041
Hemorrhage may be seen occasionally, a finding that can help differentiate toxoplasmosis from lymphoma, which typically does not hemorrhage before treatment (52).

Page 2045
Dilated perivascular spaces resulting from the presence of gelatinous pseudocysts are a frequent finding, and their presence in an immunocompromised patient should raise a red flag (Fig 11c).

Page 2049
The presence of hemorrhage associated with the lesions and intraparenchymal hemorrhage in an immunocompromised patient should cause one to consider the possibility of aspergillosis (Fig 17).

RadioGraphics 2008

This is your reprint order form or pro forma invoice

(Please keep a copy of this document for your records.)

Reprint order forms and purchase orders or prepayments must be received 72 hours after receipt of form either by mail or by fax at 410-820-9765. It is the policy of Cadmus Reprints to issue one invoice per order. **Please print clearly**.

Author Name _____
Title of Article _____
Issue of Journal_____ Reprint # _____ Publication Date _____
Number of Pages_____ KB # _____ Symbol RadioGraphics
Color in Article? Yes / No (Please Circle)

Please include the journal name and reprint number or manuscript number on your purchase order or other correspondence.

Order and Shipping Information

Reprint Costs **(Please see page 2 of 2 for reprint costs/fees.)**

_____ Number of reprints ordered $_____
_____ Number of color reprints ordered $_____
_____ Number of covers ordered $_____
Subtotal $_____
Taxes $_____

(*Add appropriate sales tax for Virginia, Maryland, Pennsylvania, and the District of Columbia or Canadian GST to the reprints if your order is to be shipped to these locations*.)

First address included, add $32 for each additional shipping address $_____

TOTAL $_____

Shipping Address **(cannot ship to a P.O. Box) Please Print Clearly**

Name _____
Institution _____
Street _____
City _____ State _____ Zip _____
Country _____
Quantity_____ Fax _____
Phone: Day _____ Evening _____
E-mail Address _____

Additional Shipping Address* **(cannot ship to a P.O. Box)**

Name _____
Institution _____
Street _____
City _____ State _____ Zip _____
Country _____
Quantity _____ Fax _____
Phone: Day _____ Evening _____
E-mail Address _____

** Add $32 for each additional shipping address*

Payment and Credit Card Details

Enclosed: Personal Check _____
Credit Card Payment Details _____
Checks must be paid in U.S. dollars and drawn on a U.S. Bank.

Credit Card: __ VISA __ Am. Exp. __ MasterCard
Card Number _____
Expiration Date_____
Signature: _____

Please send your order form and prepayment made payable to:

Cadmus Reprints
P.O. Box 751903
Charlotte, NC 28275-1903

Note: Do not send express packages to this location, PO Box.
FEIN #:541274108

Invoice or Credit Card Information

Invoice Address Please Print Clearly
Please complete Invoice address as it appears on credit card statement

Name _____
Institution _____
Department _____
Street _____
City _____ State _____ Zip _____
Country _____
Phone _____ Fax _____
E-mail Address _____

Cadmus will process credit cards and *Cadmus Journal Services* will appear on the credit card statement.

If you don't mail your order form, you may fax it to 410-820-9765 with your credit card information.

Signature _____ Date _____

Signature is required. By signing this form, the author agrees to accept the responsibility for the payment of reprints and/or all charges described in this document.

RB-9/26/07

RadioGraphics 2008

Black and White Reprint Prices

Domestic (USA only)						
# of Pages	50	100	200	300	400	500
1-4	$221	$233	$268	$285	$303	$323
5-8	$355	$382	$432	$466	$510	$544
9-12	$466	$513	$595	$652	$714	$775
13-16	$576	$640	$749	$830	$912	$995
17-20	$694	$775	$906	$1,017	$1,117	$1,220
21-24	$809	$906	$1,071	$1,200	$1,321	$1,471
25-28	$928	$1,041	$1,242	$1,390	$1,544	$1,688
29-32	$1,042	$1,178	$1,403	$1,568	$1,751	$1,924
Covers	$97	$118	$215	$323	$442	$555

International (includes Canada and Mexico)						
# of Pages	50	100	200	300	400	500
1-4	$272	$283	$340	$397	$446	$506
5-8	$428	$455	$576	$675	$784	$884
9-12	$580	$626	$805	$964	$1,115	$1,278
13-16	$724	$786	$1,023	$1,232	$1,445	$1,652
17-20	$878	$958	$1,246	$1,520	$1,774	$2,030
21-24	$1,022	$1,119	$1,474	$1,795	$2,108	$2,426
25-28	$1,176	$1,291	$1,700	$2,070	$2,450	$2,813
29-32	$1,316	$1,452	$1,936	$2,355	$2,784	$3,209
Covers	$156	$176	$335	$525	$716	$905

Minimum order is 50 copies. For orders larger than 500 copies, please consult Cadmus Reprints at 800-407-9190.

Reprint Cover

Cover prices are listed above. The cover will include the publication title, article title, and author name in black.

Shipping

Shipping costs are included in the reprint prices. Domestic orders are shipped via UPS Ground service. Foreign orders are shipped via a proof of delivery air service.

Multiple Shipments

Orders can be shipped to more than one location. Please be aware that it will cost $32 for each additional location.

Delivery

Your order will be shipped within 2 weeks of the journal print date. Allow extra time for delivery.

Color Reprint Prices

Domestic (USA only)						
# of Pages	50	100	200	300	400	500
1-4	$223	$239	$352	$473	$597	$719
5-8	$349	$401	$601	$849	$1,099	$1,349
9-12	$486	$517	$852	$1,232	$1,609	$1,992
13-16	$615	$651	$1,105	$1,609	$2,117	$2,624
17-20	$759	$787	$1,357	$1,997	$2,626	$3,260
21-24	$897	$924	$1,611	$2,376	$3,135	$3,905
25-28	$1,033	$1,071	$1,873	$2,757	$3,650	$4,536
29-32	$1,175	$1,208	$2,122	$3,138	$4,162	$5,180
Covers	$97	$118	$215	$323	$442	$555

International (includes Canada and Mexico))						
# of Pages	50	100	200	300	400	500
1-4	$278	$290	$424	$586	$741	$904
5-8	$429	$472	$746	$1,058	$1,374	$1,690
9-12	$604	$629	$1,061	$1,545	$2,011	$2,494
13-16	$766	$797	$1,378	$2,013	$2,647	$3,280
17-20	$945	$972	$1,698	$2,499	$3,282	$4,069
21-24	$1,110	$1,139	$2,015	$2,970	$3,921	$4,873
25-28	$1,290	$1,321	$2,333	$3,437	$4,556	$5,661
29-32	$1,455	$1,482	$2,652	$3,924	$5,193	$6,462
Covers	$156	$176	$335	$525	$716	$905

Tax Due

Residents of Virginia, Maryland, Pennsylvania, and the District of Columbia are required to add the appropriate sales tax to each reprint order. For orders shipped to Canada, please add 7% Canadian GST unless exemption is claimed.

Ordering

Reprint order forms and purchase order or prepayment is required to process your order. Please reference journal name and reprint number or manuscript number on any correspondence. You may use the reverse side of this form as a proforma invoice. Please return your order form and prepayment to:

Cadmus Reprints
P.O. Box 751903
Charlotte, NC 28275-1903

Note: Do not send express packages to this location, PO Box.
FEIN #:541274108

Please direct all inquiries to:

Rose A. Baynard
800-407-9190 (toll free number)
410-819-3966 (direct number)
410-820-9765 (FAX number)
baynardr@cadmus.com (e-mail)

Reprint Order Forms and purchase order or prepayments must be received 72 hours after receipt of form.